Programme Area: Energy Storage and Distribution

Project: Consumers, Vehicles and Energy Integration (CVEI)

Title: D3.2. Battery State of Health Model

Abstract:

This report represents Deliverable D3.2, Battery State of Health Model. The purpose of this report is to describe the development and validation of an algorithm that quantifies battery ageing based on input parameters that can be either inferred from Electric Vehicle (EV) usage or measured on-board. A battery is assumed to reach its (automotive) end of life when its State of Health (SOH), defined as the ratio of its measured capacity to its capacity when new, decreases to 80%. Example outputs have been generated in order to show how the algorithm can be used to assess the impact of different levels of integration of EVs into the electricity grid on battery life (and thus vehicle economics). Note that the report does not aim to present a comprehensive analysis of all combinations (which can be carried out by model users), but rather to explain how the algorithm was developed. The work reported in this deliverable forms part of the "Vehicle Energy Management Systems and Technologies" work carried out in Stage 1 of the project. The separate spreadsheet (accompanying this report) provides more detail in the form of the Battery State of Health Model itself. It should be noted that the project team had difficulties delivering the full functionality specified for this deliverable. Consequently, this model provides a relatively high-level overview of battery degradation and state of health, which will be further developed during Stage 2 of the project.

Context:

The objective of the Consumers, Vehicles and Energy Integration project is to inform UK Government and European policy and to help shape energy and automotive industry products, propositions and investment strategies. Additionally, it aims to develop an integrated set of analytical tools that models future market scenarios in order to test the impact of future policy, industry and societal choices. The project is made up of two stages:

• Stage 1 aims to characterize market and policy frameworks, business propositions, and the integrated vehicle and energy infrastructure system and technologies best suited to enabling a cost-effective UK energy system for low-carbon vehicles, using the amalgamated analytical toolset.

• Stage 2 aims to fill knowledge gaps and validate assumptions from Stage 1 through scientifically robust research, including real world trials with private vehicle consumers and case studies with business fleets. A mainstream consumer uptake trial will be carried out to measure attitudes to PiVs after direct experience of them, and consumer charging trials will measure mainstream consumer PiV charging behaviours and responses to managed harging options.

elementenergy

Project: Consumers, Vehicles and Energy Integration

Project ID: TR1006

Deliverable D3.2:

Battery State of Health Model

for

ETI

Version 4

31/01/2017

Element Energy Limited
Terrington House,

13-15 Hills Road

Cambridge, CB2 1NL

Tel: 01223 227764

Executive Summary

This report forms part of Work Package 3, "Vehicle Energy Management Systems and Technologies" of the Consumers, Vehicles and Energy Integration (CVEI) Project. An Excel model and the accompanying user manual are delivered as part of Deliverable 3.2 along with this report.

This report describes the development and validation of an algorithm that quantifies battery ageing based on input parameters that can be either inferred from Electric Vehicle (EV) usage or measured on-board. A battery is assumed to reach its (automotive) end of life when its State of Health (SOH), defined as the ratio of its measured capacity to its capacity when new, decreases to 80%. Example outputs have been generated in order to show how the algorithm can be used to assess the impact of different levels of integration of EVs into the electricity grid on battery life (and thus vehicle economics). Note that the report does not aim to present a comprehensive analysis of all combinations (which can be carried out by model users), but rather to explain how the algorithm was developed.

A brief review of the academic literature is presented, discussing the principles underlying the ageing of automotive batteries. Battery ageing manifests itself in the form of capacity fade and resistance rise during storage and cycling. Whilst these processes are linked, the capacity fade was found to be the most significant contributor to battery ageing. The principal phenomena that underpin capacity fade are discussed in this report.

Two principal components of battery ageing are explained in the report; calendar damage, degradation that proceeds with time; and cycling damage, degradation that is caused by charging and discharging the battery. Phenomena that underpin calendar ageing were found to be linked to the processes that occur on the anode (negative electrode) and do not strongly depend on the cathode chemistry (positive electrode). On the other hand, cycling ageing is a more complex process and can proceed at different rates depending on the cathode active material. Thus, cathode-specific coefficients for cycling ageing have been developed using information reported by battery manufacturers.

The ageing algorithm described in this report is incorporated into the accompanying Excel-based tool. The extent to which different factors influence battery ageing are discussed in the report. Experimental evidence from peer-reviewed publications is presented to support the choice of inputs and calibration of the algorithm. The following operational parameters have been found to have the largest impact on battery degradation and were included in the model:

- Temperature (strong impact on both calendar and cycling ageing – degradation increases with temperature)
- state of charge (medium impact on calendar ageing – degradation increases when stored at high state of charge)
- Time (high impact on calendar ageing – degradation increases with time)
- Current throughput (high impact on cycling ageing – degradation increases with current throughput)
- Depth of Discharge window (strong impact on cycling ageing – degradation is higher for cycling within a large depth of discharge window)
- Rate of (dis)charge (limited impact on cycling ageing – increases with the rate of (dis)charge)
- Cathode chemistry (strong impact on cycling ageing)

Assuming a London temperature profile[1], a typical lithium-ion battery will experience approximately 1% calendar degradation per year almost irrespective of the usage profile. The cycling ageing is in addition to calendar degradation and is heavily dependent on specific battery chemistry and cycling conditions. Assuming a typical travel distance of ca. 15,000 km per year, the cycling ageing can range from less

[1] The maximum monthly average temperature is 23.7°C and the minimum monthly average temperature is 8.0°C in London based on the Met office data in 2015.

than 0.2% per year, for a PHEV used predominantly (90% of all travelled distance) in charge sustain mode, to ca. 1% per year, for a BEV. Thus, the lifetime of a typical BEV battery is close to 10 years (but can be substantially lower or higher depending on the specific usage profile and the battery chemistry) and the lifetime of a PHEV battery can easily exceed 10 years if the PHEV is used in a mixture of charge depleting ('electric mode') and charge sustaining modes.

The effect of managed charging is modelled through changes in the state of charge and the rate of charge. The potential effect of other parameters is also discussed in the report. The impact of managed charging results in up to 12.5% decrease in a battery lifetime in the example cases presented, but equally may lead to an increase in battery lifetime if optimised with battery degradation in mind (by minimising the time spent at high SOC). The provision of Vehicle to Grid services (whereby power from the battery is fed back into the grid) is modelled through increased battery cycling within a specified Depth of Discharge. The effect of additional cycles causes up to almost 40% decrease in battery lifetime in the example cases discussed. The analysed case studies indicate potential entry points for EV integration into the electricity grid – for example providing delayed-start managed charging, or participating in V2G services, but limiting the power and the Depth of Discharge window when providing the services.

Results of EV user surveys (for the BYD e6, Nissan Leaf, Tesla Roadster and Tesla Model S) are discussed in the report and are in line with the model predictions. However, it was concluded that results from EVs tested in a controlled environment are necessary to validate of the model. Hence, the model was validated with the battery degradation data collected from on-road EVs, specifically Nissan Leaf (BEV), Toyota Prius (PHEV) and Chevrolet Volt (PHEV).

No single model available in the literature was found to satisfactorily predict all battery degradation phenomena and allow full flexibility in terms of battery chemistry and manufacturing technique. Therefore, this report also aims to clearly explain the caveats and limitations of the developed semi-empirical modelling approach. The developed model intends to provide a sufficiently accurate battery lifetime prediction in order to estimate the feasibility of managed charging and Vehicle to Grid services. However, the model (like any other semi-empirical model) cannot be used to develop new battery chemistries and is not intended to provide sufficiently high accuracy to be applied in real-time SOH calculations on-board of a vehicle.

Contents

This report is produced under the Consumers, Vehicles and Energy Integration project, commissioned and funded by the ETI.

Authors

This report has been prepared by Element Energy. For comments or queries please contact:

Celine Cluzel celine.cluzel@element-energy.co.uk 0330 119 0984

Vlad Duboviks vlad.duboviks@element-energy.co.uk 0330 119 0995

Reviewers

This report has been reviewed by:

Alex Stewart, Associate Director, Element Energy
Richard Riley, Consultant, Element Energy
Foaad Tahir, Senior Consultant, Element Energy (Annex)
Dave Densley, TRL Associate, TRL
Colin Ferguson, CEO, Route Monkey
Osama Khalifa, Data Analyst, Route Monkey
Thi Minh Phuong Nguyen, Research Engineer, EDF energy
Thierry Brincourt, EV Project Manager, EDF energy

Version control

Version number	Submission date	Comments
1	25/04/2016	First version
2	20/10/2016	Revised version
3	16/12/2016	Revised version
4	31/01/2017	Revised version (mostly addition of the annex)

Acknowledgements

We would like to acknowledge the contributions of Professor David Greenwood, who shared his expertise and insights into the automotive battery industry during the discussion at the Warwick Manufacturing Group centre. We are also grateful to Colin Ferguson and Osama Khalifa at Route Monkey for sharing their technical expertise in developing State of Health models and reviewing this report. We would also like to thank Thi Minh Phuong Nguyen and Thierry Brincourt from EDF for reviewing the report and providing useful suggestions and comments. Finally, we would like to thank the researchers at the Idaho National Laboratory for providing detailed answers to our queries regarding the on-road Electric Vehicle data published on their website.

Acronyms

Ah	Ampere hours
BEV	Battery Electric Vehicle
BMS	Battery Management System
CV EI	Consumers, Vehicles and Energy Integration
DNO	Distribution Network Operator
DOD	Depth of Discharge
EV	Electric Vehicle
FFR	Firm Frequency Response
INL	Idaho National Laboratory
LAM	Loss of Active Material
LCO	Lithium Cobalt Oxide
LFP	Lithium Iron Phosphate
Li	Lithium
LLI	Loss of Lithium Inventory
LMO	Lithium Manganese Oxide
LTO	Lithium Titanium Oxide
NCA	Lithium Nickel Cobalt Aluminium Oxide
NMC	Lithium Nickel Manganese Cobalt Oxide
OEM	Original Equipment Manufacturer
PHEV	Plug-in Hybrid Electric Vehicle
Q	Capacity
RPM	Revolution Per Minute
SEI	Solid Electrolyte Interphase
SOC	State of Charge
SOH	State of Health
STOR	Short Term Operating Reserve
ToU	Time of Use
V2G	Vehicle to Grid

Note on terminology

Thorough the report, ‘EV’ refers to a plug-in vehicle, which can be either a PHEV or BEV.

1 Introduction and scope

1.1 ETI Consumers, Vehicles and Energy Integration project

The overall aim of the Consumers, Vehicles and Energy Integration (CVEI) Project is to provide a detailed understanding of how the UK's car and van markets and related refuelling infrastructure will need to evolve in the future in order to meet long term CO_2 reductions from the transport sector. In particular, it aims to define internally consistent future scenarios which take account of changes in vehicle technologies and costs, consumer behaviour, policy and evolving commercial models. Given the likely role of electrified powertrains in the future light vehicle parc, a key focus of the project is the interaction between vehicles and the electricity system (in addition to hydrogen and existing liquid fuel infrastructure), both from a technical point of view and in terms of the roles for different actors at each part of the value chain such as electricity suppliers, grid operators and vehicle manufacturers. During Stage 1, the project has developed an overarching 'analytical framework', a collection of models and tools to quantify these future scenarios and assess their relative strengths. Stage 1 will also map potential configurations for 'managed charging' of electric vehicles to minimise negative impacts on the wider electricity system (and potentially to provide a net benefit). Some of these technical and commercial configurations will be tested in real-world vehicle and charging trials in Stage 2 of the project.

This report forms part of Work Package 3, entitled Vehicle Energy Management Systems and Technologies. The battery pack is a key component of electric vehicles (EVs), and the development of its cost and performance attributes over time will have a critical influence on future uptake and use of electric vehicles. This component is also the link between EVs and the wider energy system and it has the potential to create new services that benefit several actors across the energy supply value chain (e.g. grid services aggregators, charging infrastructure operators, energy suppliers). For this reason, vehicle battery packs are the primary focus of WP3. Specifically, the scope includes a technology roadmap of battery costs and performance up to 2050, which provides a complete set of projections for use in vehicle uptake models in Work Package 1; secondly, it includes an assessment of Battery Management Systems (BMS), their current features and potential additional capabilities required to provide tighter integration with the electricity system (and hence opportunities for research and development to address these gaps); finally, the development of an Excel-based State of Health (SOH) model providing evidence on the impact of different battery use patterns on battery life. This report, Deliverable 3.2, covers the development of an Excel-based State of Health model.

1.2 Objectives and scope of the work

The purpose of this deliverable is to develop an algorithm to quantify the state of health (SOH) of a given battery from the data available while it is in use in a vehicle. SOH is a complex metric that reflects the ability of the battery to deliver the specified performance and takes into account its capacity, internal resistance, voltage and self-discharge. However, most commonly it is defined as the capacity at the time of the measurement as a proportion of the starting capacity [1]; this definition has been adopted for this report. The algorithms described in the report are incorporated into a simple model that simulates battery ageing based on a number of input parameters. The tool is also able to quantify the performance and cost impact of demand management strategies on automotive batteries.

The developed algorithm uses parameters that can be monitored during the Stage 2 Trial.

The scope of the model includes current lithium-ion battery technologies, but excludes future chemistries, such as lithium-air and lithium-sulphur. These chemistries have not yet demonstrated sufficiently long cycle life for automotive applications (refer to report D3.1 for more detail on the current state of development and projected performance). Therefore, if these technologies do enter the automotive market, they will have different cycling and ageing characteristics than the prototype being

tested in laboratories today. For this reason, a State of Health model cannot be parameterised and calibrated for future technologies.

The report also aims to assess the potential impact of EV integration in the electricity grid on battery lifetime, allowing the impacts of the different demand management strategies to be tested and highlighting mitigation strategies to minimise impacts and maximise revenues for vehicle users, fleet operators and other relevant actors.

Under Deliverable 3.2, the following deliverables have been developed:

- An Excel based model of lithium-ion battery state of health that can quantify the performance and cost impact of demand management strategies
- A user manual for the above model
- A report laying out how the model equations have been derived and validated – this is the present report.

1.3 Approach and structure of the report

The report is structured into six chapters with Chapter 2 and Chapter 3 discussing the details of the modelling approach.

Chapter 2 presents the methodology for estimating SOH, including the underlying ageing phenomena and the key parameters affecting the rate of degradation. It also includes a short review of battery degradation studies in academic literature. Battery degradation is discussed at a cell level in this chapter. The choice of model parameters is explained and the modelling results are validated against several literature sources.

Chapter 3 is focused on the analysis of the results on a pack level and discusses the results of EV user surveys and on-road EV testing.

Chapter 4 presents the summary of the results and identifies data gaps. The bibliography is included in Chapter 5.

An Annex in Chapter 6 describes how the CVEIP Phase 2 trial data will be sued in the State of Health Model.

2 Development of the approach to model automotive battery ageing

2.1 Underlying principles

Battery ageing is a complex process that depends on multiple parameters and can proceed through a number of different pathways. To estimate the lifetime of a battery it is necessary to establish a link between measurable parameters and the underlying ageing mechanisms. This may also depend on the specific battery chemistry. At present, the positive electrode materials used in commercial lithium ion batteries mainly include $LiMn_2O_4$ (LMO), $LiFePO_4$ (LFP), $LiNi_xCo_yMn_{1-x-y}O_2$ (NMC) and $LiNi_xCo_yAl_{1-x-y}O_2$ (NCA) and the most commonly used negative electrode material is graphite [2]. Ageing phenomena that dominate early-stage degradation in such batteries occur at the interface between the negative electrode and the electrolyte [2], [3].

Being outside of the stability window of organic electrolytes, the negative graphite electrode promotes electrolyte reduction during the first few battery cycles [4]. The accompanying side-reactions lead to the formation of inorganic lithium (Li) compounds (e.g. Li_2CO_3) [5]. As a result, a Solid Electrolyte Interphase (SEI) is formed between the negative electrode and the electrolyte. SEI effectively passivates the electrode and prevents further electrolyte reduction and corrosion of Li and the electrode. However, dynamic electrochemical conditions within the cell can destabilise the SEI and cause the corrosion of Li to proceed. This results in battery capacity loss and is termed Loss of Lithium Inventory (LLI).

A common degradation mechanism that is more pronounced at later stages of a battery's lifetime is the Loss of Active Material (LAM). Positive electrodes in lithium batteries are composite structures that contain lithium compounds (e.g. $LiFePO_4$) as well as carbon additives that improve electrical conductivity. Carbon rearrangement within the positive electrode during the battery lifetime, can lead to deterioration of electronic contact and thus deactivation of parts of the electrode [6]. Additionally, certain electrolytes containing acidic species have a tendency to form highly resistive surface films on positive electrodes leading to further deactivation of the electrode [7].

Both LLI and LAM have a complex dependence on a number of battery parameters. Factors with the highest impact on degradation are (a) temperature, (b) state of charge (SOC) (c) charge/discharge rate and (d) charge/discharge window [8]. High temperatures can promote electrode decomposition leading to SEI growth and higher activity leading to resistive film formations on positive electrodes contributing to LAM. High SOC during storage promotes chemical reactions of electrode/electrolyte interface and leads to higher lithium loss. The speed of charge/discharge is typically denoted as C-rate[2] and has a potential to influence the lifetime of a battery through kinetic effects. Charge/discharge window is typically referred to as Depth of Discharge (DOD) and affects electrolyte stability and structural robustness of the electrodes. In addition to LLI and LAM, multiple other phenomena have the potential to contribute to degradation in specific conditions, e.g. lithium plating leads to accelerated degradation at near-zero temperatures and graphite exfoliation degrades the negative electrode when the cell is operated at a high voltage.

2.2 Approach to battery lifetime predictions

Battery SOH can be estimated through (a) fundamental physics-based models or (b) semi-empirical models relying on experimental data. Development of an accurate *ab initio* model that considers all degradation effects is extremely challenging because of the complex relationship between battery characteristics and the ageing mechanisms. Not all of the battery degradation mechanisms are currently understood, further complicating the development of degradation models relying on the simulation of physical processes. The alternative approach is to predict degradation by using semi-empirical models

[2] If the battery is fully discharged from 100% in one hour the C-rate is 1C. A C-rate below 1C means that the drawn current is below the rated capacity of the cell. Drawing a current at C-rate above 1C will cause the cell to discharge at a 1/C-rate fraction of an hour, e.g. 2C means the battery would be discharged in 30 mins. A Nissan Leaf charging at 50 kW corresponds roughly to a 2C charging.

that are parameterised using experimental results. This approach inevitably leads to a number of assumptions that may not always reflect real-life operational conditions. The main limitations of such models are as follows:

- Use of averaged values for some inputs. This assumes that batteries are exposed to static conditions.
- Extrapolation of single cell laboratory testing results to multiple-cell battery packs. This ignores thermal gradients and cell imbalances that may develop inside battery packs.
- Extension of experiments conducted on specific cells to other cell sizes and manufacturers. Specifically, most of the academic literature reports the results for 1-3Ah cylindrical cells, while car manufacturers typically use >40Ah cells. Note that this limitation is addressed by calibrating equations using manufacturer's data for larger cells – refer to Section 2.4.4.
- Ignoring a number of parameters, such as the type of electrolyte, type of battery separators, as well as the presence of vibration during use. Each of these factors may have only a minor effect on degradation, but combined these may cause noticeable deviations from the expected result. However, it is not practical to include all of these parameters in a semi-empirical model, as each additional parameter multiplies the number of required experiments by at least a factor of 3.

The semi-empirical modelling approach will be explained in detail in this report. Despite certain limitations, semi-empirical models offer a useful way of estimating battery lifetime using relatively simple inputs that can be measured on-board a vehicle by a standard Battery Management System (BMS) and do not require special equipment. For a realistic lifetime prediction, it is useful to separate battery degradation into calendar and cycling degradation. Calendar degradation refers to the degradation mechanisms that happens through time, even when the battery is not in use, while cycling degradation happens when the battery is used.

Calendar damage was found to be proportional to the square root of time and is a function of temperature and SOC. Cycling damage depends on the current throughput [8] and is a function of temperature, C-rate, DOD and the cathode chemistry. The impact of each parameter depends on other inputs, e.g. SOC may have a higher impact on battery life in EVs with low annual mileage, when calendar degradation exceeds cycling degradation, while the choice of cathode material may be more important in EVs with high annual mileage because this will have high impact on cycling ageing.

2.3 Calendar ageing analysis and model calibration

2.3.1 Calendar ageing equation

A calendar ageing equation can be derived based on the assumption that degradation occurs due to lithium corrosion at the SEI layer, i.e. LLI mechanism due to SEI evolution as discussed in Section 2.1. Broussely et al. hypothesised that the corrosion rate depends linearly on the thickness of the SEI [5]. This leads to the following relation between time *t* and the amount of Li corroded *x*:

$$t = Ax^2 + Bx$$

The Arrhenius equation, a commonly used empirical relation that links reaction rates to temperature, suggests exponential dependence of reaction rate on temperature. Broussely et al. derived the following coefficients by combining this assumption with the experimental results (where T is the temperature in Kelvin):

$$A = e^{\frac{4661}{T} - 14}$$

$$B = e^{\frac{4437}{T} - 11.6}$$

The capacity loss is obtained by expressing x in terms of *t* from the equation above. As mentioned in Section 2.2, the capacity loss is dependent on the square-root of time. Although this type of dependency

was originally developed for $LiCoO_2$ (LCO) batteries [5], it has been successfully tested and validated for other chemistries, including LFP [9] and NMC [10]. As long as the relationship describes LLI that occurs at the negative electrode, it is reasonable to assume that it will hold for all chemistries that use graphite electrodes. However, the A and B coefficients developed by Broussely et al. back in 2001 may not be accurate for characterising current state of the art cells. Therefore, the coefficients have been adjusted to achieve a good fit for current state of the art cells as shown in Figure 1, the adjusted coefficients are:

$$A = e^{\frac{8000}{T} - 24.2}$$

$$B = e^{\frac{4437}{T} - 15}$$

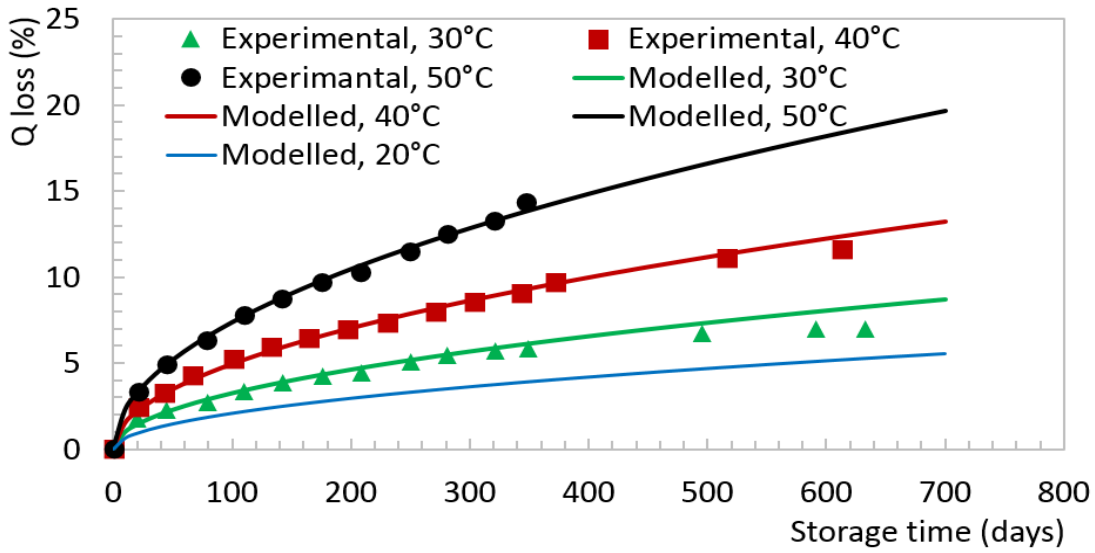

Figure 1 Validation of the capacity loss curves with experimental data for calendar ageing at different temperatures obtained from state-of-art LFP cells by Sarasketa-Zabala et al. at 70% SOC. Adapted from [9]

The experimental data in Figure 1 correspond to static temperature conditions. However, in order to be able to model degradation in real-life, the model should provide the facility to use variable temperature inputs. Extrapolation of the results of static experiments to the modelling of dynamic conditions introduces uncertainty. However, it is recognised that inaccuracies due to the use of average values for temperature may be greater than the uncertainty introduced by the use of dynamic values (although this cannot be quantified due to the lack of data). Therefore, temperature has been made dynamic in the model through the introduction of annual temperatures profiles using monthly average temperatures.

2.3.2 Effect of the state of charge (SOC)

E.ON has previously conducted research that analysed the sensitivity of PHEV batteries with NMC cathodes to the SOC, in the context of controlled and uncontrolled charging. High battery SOC was found to increase the degradation rate [11]. The influence of state of charge on calendar ageing was found to correlate with the graphite electrode potential in NMC batteries [10]. This suggests that this dependency is likely to be valid for other battery chemistries employing negative graphite electrodes (positive electrodes can be LMO, LFP, NMC, NCA, etc.)

The model has been calibrated for SOC degradation using a recent study of LFP batteries [9]. Results of the study suggest an exponential relationship between SOC and battery lifetime, which is in line with the results of experiments with NMC batteries [12]. Both the LFP and NMC studies suggest that a

battery stored at 40°C with a SOC of 50% will have double the lifetime of a battery stored with a SOC of 90% [9,12]. Based on the results of these studies and the information available on the origins of the SOC effect on degradation, the SOH model assumes the same calendar ageing dependency on SOC for all modelled battery chemistries.

Although the evidence presented in recent literature suggests that storage SOC is of secondary importance compared to storage temperature [13], [14], this effect cannot be ignored. SOC is therefore explicitly added into the calendar ageing equation as a pre-exponential factor. The modified equation is calibrated with the data from the same publication that was used for temperature calibration (Figure 1) for consistency. This is shown in Figure 2.

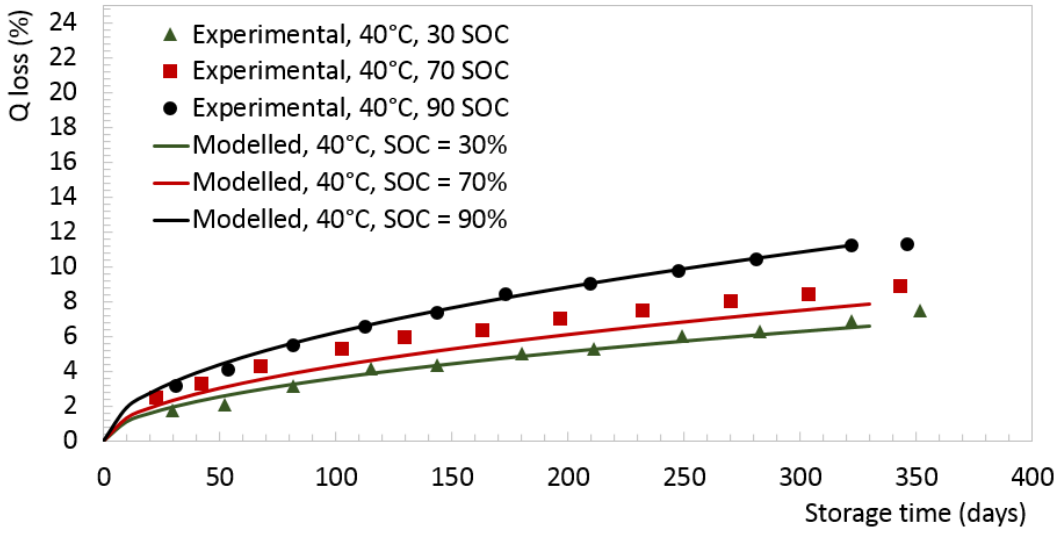

Figure 2 Validation of the capacity loss curves with experimental data for calendar ageing at different SOC obtained from state-of-art LFP cells by Sarasketa-Zabala et al. at 40 °C. Adapted from [9]

2.3.3 Limitations of the calendar ageing equation

In summary, the caveats of using the developed relationship are:

- The model has been validated using experimental results for temperatures equal to or higher than 30°C. There is no reason to expect noticeable changes in the relationship at lower temperatures (e.g. 15-25°C), however the data for temperatures below 30°C was not available from peer-reviewed publications used for the model calibration. Note that some battery manufacturer data is available at room temperature and is discussed in Section 2.4.4.
- The model has been calibrated using the results of "static" experiments available in the literature, i.e. experiments where a particular type of battery has been tested varying only one degree of freedom, e.g. temperature, while keeping all other parameters constant. Results available from different sources have been combined in the model, allowing the model to take all of the key parameters into account. The limitation of this approach is the assumption that all interdependencies are linear.
- The use of average inputs in the model for some parameters (e.g. SOC) reflects the fact that the equations have been parametrised using experiments where these inputs have been held constant. As long as a semi-empirical approach to modelling is used, the equations do not describe physical processes that lead to degradation, but instead reflect the observed response of the system to the testing conditions. It is therefore unclear whether dynamic testing conditions will result in a different response, compared to the static conditions used for model parameterisation. Average values of SOC are therefore used in the model.

- The calendar ageing mechanism of different types of batteries depends on the negative and positive electrode material type. However, calendar ageing was found to be dominated by the degradation of the negative electrode. As most automotive batteries use graphite for the negative electrode, no significant differences in calendar ageing between these chemistries is expected. However, it is recognised that different types of chemistries may lead to certain variations in lifetime that are not captured by the model due to the lack of available data.

2.4 Cycling ageing analysis and model calibration

Cycling ageing is more complex to model as it does not rely on a single dominant degradation mechanism. Cycling ageing depends on several independent variables that are related both to the external conditions as well as battery utilisation profiles [3]. Depending on the specific duty cycle, the cycling ageing scenarios can include any combination of LAM, LLI, kinetic degradation, increase in polarisation resistance and the formation of parasitic phases [15]. Semi-empirical cycle life models are designed to fit the observed degradation data, rather than to follow a particular degradation mechanism.

In cycle models, the current throughput (Ah throughput) is chosen as the main parameter; this allows the model to quantify the effect of C-rate and DOD [16]. Typically, cycling ageing also considers the effect of temperature [17], [18]. The basic form of the equation for cycling ageing, that is used in this report, has been proposed and validated for LFP batteries [16], as well as NMC batteries [19]:

$$Q_{cycle\ loss} = B \cdot exp\left(\frac{E_a}{RT}\right)(Ah)^z$$

$Q_{cycle\ loss}$ - capacity loss due to battery cycling, B – pre-exponential factor that depends on the C-rate, E_a – activation energy (for batteries with LFP cathodes this is equal to 31 500 J mol^{-1}), R – ideal gas constant equal to 8.314 J K^{-1} mol^{-1}, T – temperature in Kelvin and z – exponential factor [16].

2.4.1 C-rate

From the cycling ageing equation, it follows that if the battery is constantly cycled at high C-rates it will undergo more cycles in a given time and consequently will have a shorter life-span. Additionally, it was observed that cells that are charged or discharged at high C-rates degrade faster compared to their counterparts charged at slower rates, even if the number of cycles is equal in both cases. I.e. smaller total amount of current can pass through the cell before it degrades below a certain threshold if cycled at high C-rates. A closer examination of C-rate effect showed that experimental data obtained at different C-rates can be fitted if E_a decreased with increasing C-rate. Wang et al. suggested to modify the equation as follows to account for the additional C-Rate effect [16]:

$$Q_{cycle\ loss} = B \cdot exp\left(\frac{-31700 + 370.3 \cdot C_{rate}}{RT}\right)(Ah)^z$$

This equation has been successfully applied to model degradation of LFP batteries in plug-in hybrid electric vehicles (PHEVs) and battery electric vehicles (BEVs) by Bishop et al. who also suggested that it is applicable to other Li-ion chemistries with similar ageing mechanisms [20]. As previously mentioned, the coefficient B is linked to the C-rate. The original paper by Wang et al. provides the values of B for four different C-Rates as shown in Figure 3. These data points were linearly approximated to develop an explicit dependency of cycling ageing on C-Rate for the model delivered as part of D3.2. Note that linear approximation has a relatively low R-squared value due to a small number of experimental data points available. However, this translates to a minor uncertainty in terms of $Q_{cycle\ loss}$ as the overall effect of C-Rate factor is relatively small.

At high C-rates, the rate of precipitates formation during the side-reactions at the electrolyte-electrode interface, including due the electrolyte decomposition, is increased. This directly contributes to faster SEI growth, thus increasing the internal resistances of the cell and perpetrating the LLI [21]. There is also an indirect effect on temperature, which increases due to both the increase in resistance and higher

rate of side-reactions. Therefore, there is a positive feedback between the C-rate and temperature. Thus, high C-rates can cause the increase in battery pack temperature with a passive air cooling and thereby affect the rate of degradation. For example, rapid charging at 50 kW was shown to increase the Nissan Leaf battery pack temperature by 6.5°C, and slow charging at 3.3 kW by 2.9°C [22]. The temperature was found to decrease back to ambient quickly after the charging event. Provided that the vehicle spends most of the time stationary, the effect of C-rate on temperature is relatively small over its lifetime. Furthermore, this effect is difficult to capture, because the increase in temperature will depend on the design of the pack and the cooling system. Therefore, the model developed as a part of this project does not aim to replicate this effect.

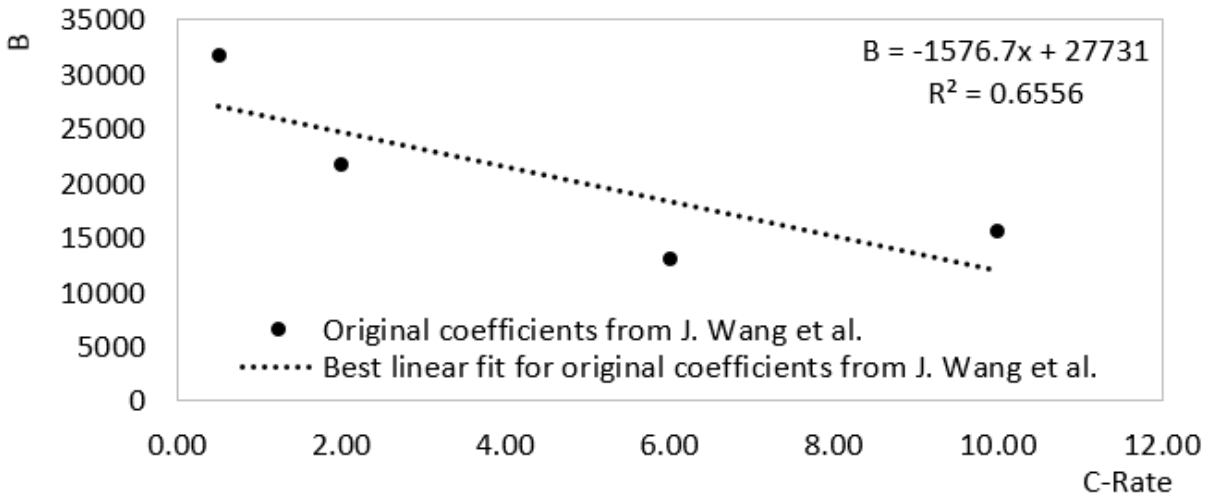

Figure 3 Calibration of C-Rate dependant coefficient B using experimental data from [16]

2.4.2 Temperature

The cycling ageing equation has been validated at a C-rate of 0.5 for different temperatures as shown in Figure 5. Note that the cycling experiments are relatively short and do not include any rest periods, therefore the calendar ageing is not relevant for the results presented in Section 2.4. Experimental data in Figure 4 comes from the testing of commercially available 26650-type[3] cylindrical cells [16]. It is clear that elevated temperature has a profound effect on degradation. This is in line with the discussion presented in Section 2.1.

[3] Battery cell with the following dimensions: 26.5 mm diameter x 65.4 mm length.

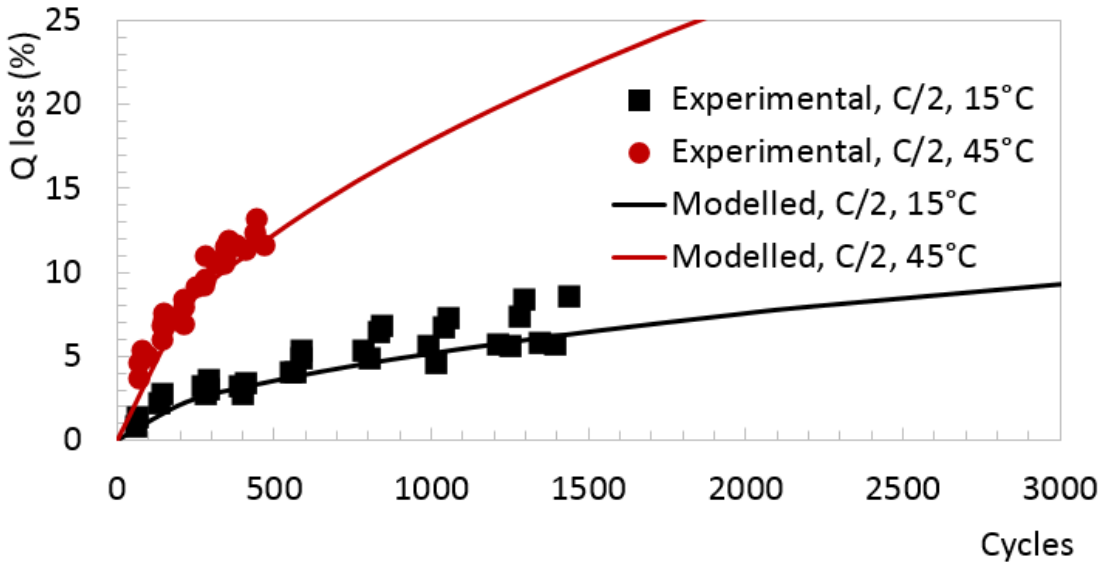

Figure 4 Cycling ageing equation validation for LFP cells at different temperatures using experimental data from Wang et al (various DOD, 50% assumed for the model). Adapted from [16]

2.4.3 Depth of Discharge (DOD)

DOD is another recurring factor in the literature that causes batteries to degrade at different rates. There is no consensus regarding the exact origins of the effect of DOD on cycling degradation. One possibility is that SEI development and LAM are accelerated under high DOD conditions [3]. It is likely that a number of underlying processes are influenced by the DOD. It was experimentally demonstrated that high DOD causes faster cycle degradation in LFP cells, albeit the effect is less pronounced than the effect of discharge rate [16]. On the other hand, a recent study recognised the effect of DOD as more significant than the C-rate and showed that higher DOD may not necessarily be more detrimental to the cell [18]. Thus, the exact relationship between capacity fade and DOD range remains unclear. However, most publications report an increase in degradation as the DOD increases [10], [17], [23]–[25]. The effect of DOD on degradation is most pronounced when the battery is cycled either at very low or at very high DOD - cycling at high DOD leads to higher degradation compared to cycling at low DOD.

The data used for modelling the effect of DOD is based on battery cycling around the SOC=50%. In practice, the EV batteries will not be cycled around 50%, so it is assumed that the effect of cycling around the SOC=50% is the same as the effect of cycling around any other SOC, provided the absolute DOD window stays the same. The data used for model calibration suggests the lowest degradation occurs at 5% DOD, in line with the commonly observed trend, and the highest degradation at 30%. It also reports that the degradation rate decreases when the DOD is increased beyond 30%, but it nevertheless remains higher than at 5% DOD [18]. Therefore, the model assumes three separate cycling ageing regimes: (a) for DOD below or equal 5%, (b) DOD between 5% and 30%, and (c) DOD above 30%. Note that the effect of DOD is modelled by varying the exponential factor *z* (see equation in Section 2.4.1).

Introduction of discrete DOD bands for cycling ageing models is not uncommon. This approach is used in the academic literature to reflect the non-linear DOD relationship with Ah-throughput [18], [26]. Calibration of the model for 0-5%, 5-30% and 30-100% bands is performed with experimental data obtained by Sarasket-Zabala et al. as shown in Figure 5 [18]. Note that the value of the factor *z,* which is around 0.5, suggests an almost square root dependence on Ah throughput.

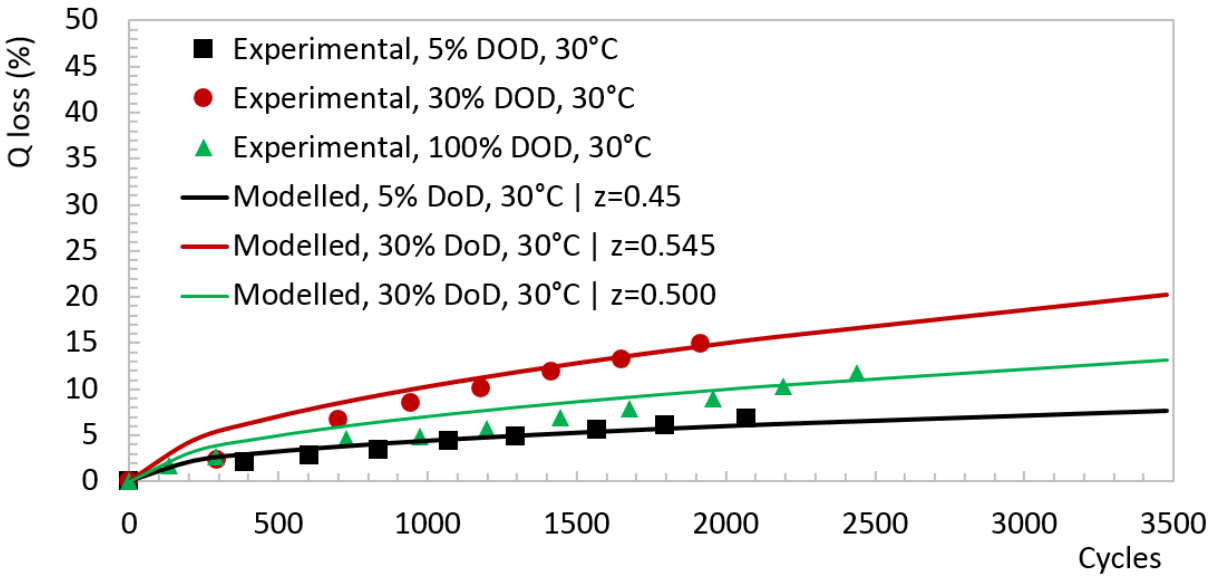

Figure 5 Validation of the cycling aging with experimental data from state-of-art LFP cells (cycling at 1C in all cases). Adapted from [18]

2.4.4 Chemistry

The cycling ageing modelling methodology is based on the results for LFP cells. The same form of equation was shown to be applicable for NMC\LMO chemistry and has been suggested to be applicable for NCA chemistries [10], [17], [18]. Although the form of relationship is expected to be the same for these chemistries (LMO, NMC, NCA), the equation still needs to be calibrated with the experimental results for each chemistry. Note that LMO electrodes have poor cycling life and therefore are typically blended with other materials (e.g. NMC) to achieve a reasonable cycling life [27], [28].

Battery cell manufacturers often publish cycling degradation of their batteries at room temperature – typically 20-23 °C and constant 80-100% DOD. Manufacturer's data at these conditions is shown in Figure 6. A good fit of modelled degradation is demonstrated for LFP cells manufactured by BYD. Manufacturer's data in Figure 6 suggests that batteries with NMC and NCA cathodes degrade at a faster rate than LFP batteries. An additional chemistry-specific factor α is introduced to the model to account for battery chemistry, and specifically for the type of cathode. The cycling equation is modified as follows to account for the degradation of different cathodes:

$$Q_{cycle\ loss} = B \cdot exp\left(\frac{-31700 + 370.3 \cdot C_{rate}}{RT}\right)(Ah)^{z+\alpha * DOD}$$

The value of α is calibrated by fitting the model results to manufacturers' data for BYD (LFP), Kokam (NMC) and Saft (NCA) cells, as shown with grey lines in Figure 6 [29]–[31]. The values of α are found to be as follows: 0 for LFP, 0.037 for NCA and 0.057 for NMC. The fact that the equation coefficients developed for cylindrical LFP cells fit the data for larger pouch-type BYD cells suggests that the size of cells does not noticeably affect the degradation. However, this direct comparison should be made with caution as no unambiguous evidence to prove this statement was found in academic literature. Modelling results were validated against data for high capacity cells suitable for automotive applications in Figure 6.

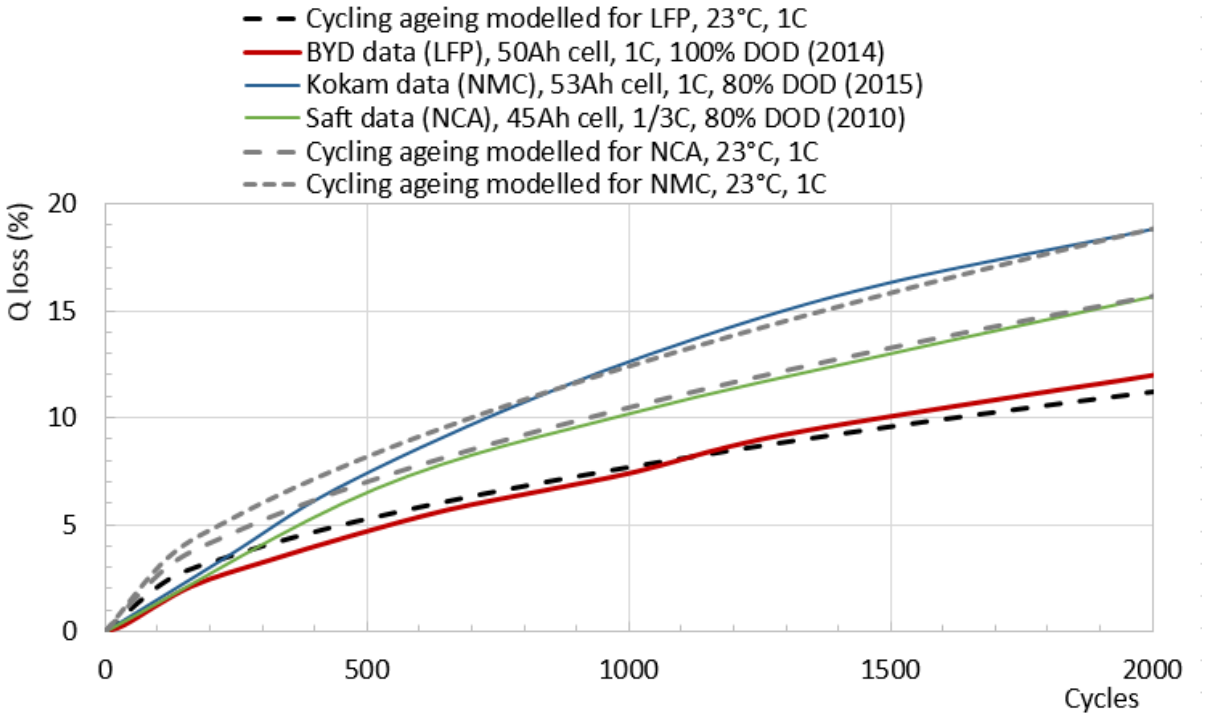

Figure 6 Validation of the modelling results with manufacturer's data for BYD (LFP), Kokam (NMC) and Saft (NCA) cells [29]–[31]**. All data is at room temperature**

2.4.5 Limitations of the cycling ageing equation

The limitations of the cycling ageing equation include some of the limitations already described for the calendar ageing equation (refer to Section 2.3.3 – specifically the uncertainty due to the use of average values (C-rate during charging and discharging)). Equally, the fact that the model is calibrated by the experimental data for static DOD experiments means that the effects that may be introduced by dynamic DOD conditions are not included. Operation under dynamic DOD conditions was shown to lessen degradation, but as the nature of this effect remains unclear this is not included in the model [18]. Additionally, it should be noted that the literature review revealed a significant uncertainty in the depth of discharge effect on degradation rate. While our analysis has made use of the most reliable data, an inherent uncertainty is associated with this relationship.

Lithium metal plating is known to occur at near-zero temperatures when cycling at high currents [32]. This result in the capacity loss due to the decrease in the loss of active material. There is little experimental data on degradation loss at near-zero temperatures preventing the model calibration for this. At the same time, extensive lithium plating is unlikely to occur in commercial EV battery packs because the OEMs either install internal battery heaters to prevent operation at near-zero temperatures or limit the current at low temperatures. It should be noted that as the operating temperatures approach near-zero values, degradation that is not captured by the developed algorithm might start to occur.

The degradation rate may vary between manufacturers even for identical chemistries. An example of the observed variations in the degradation of LFP cells produced by different manufacturers is shown in Figure 7 [29], [33]–[35]. Partly the difference can be attributed to the manufacturing quality and the use of proprietary technologies. Equally, this could be due to a number of other factors that are challenging to parametrise such as battery pack size, choice of the electrolyte, etc. These are not directly captured by the model. Larger pouch cells are known to have higher current and lithiation inhomogeneity that may affect degradation. These effects need to be considered in a physical cell model and are beyond the capability of the developed algorithm. However, in the case of the LFP chemistry the model has been calibrated using the data for cells that were designed for automotive applications. Also, the degradation of these batteries is approximately in the middle of the observed

degradation spectrum in Figure 7 (BYD data). The model also includes a functionality to specify a custom chemistry-specific factor, which could be used to calibrate the model with the data for any specific cell.

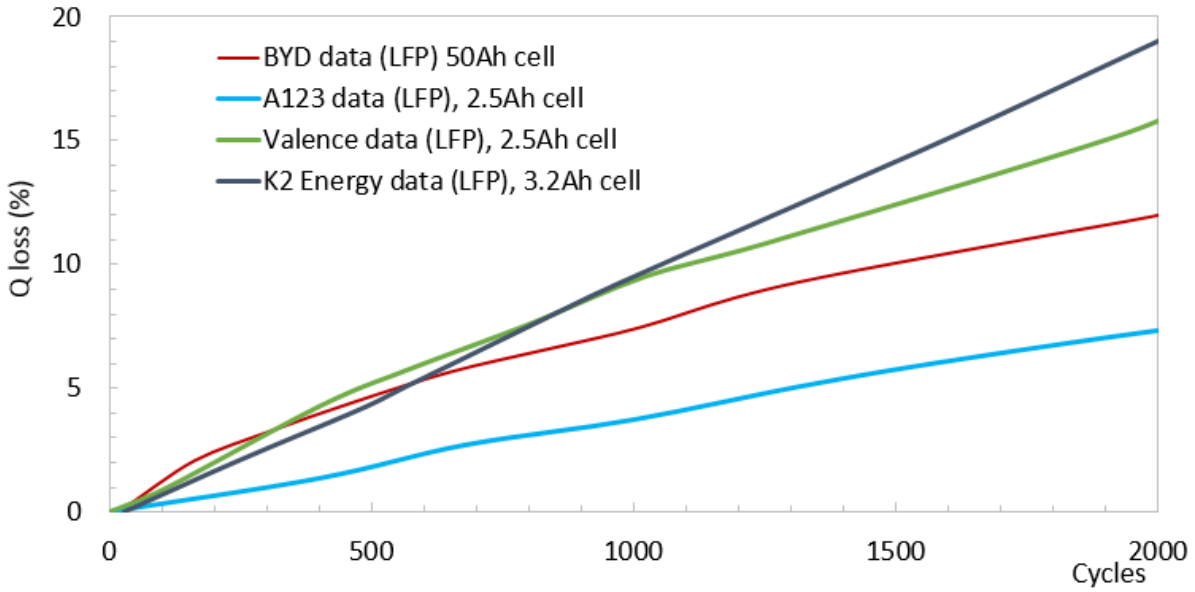

Figure 7 Cycling degradation reported by different manufacturers of LFP batteries for the same conditions – room temperature, 100% DOD and 1C [29], [33]–[35]

Chemistry-specific factors have been calibrated at room temperature and 100% DOD as the manufacturers' spreadsheets report degradation for these conditions only. It is therefore assumed that the relationship holds for all other conditions. It is recognised that batteries with different chemistries may respond slightly differently to changes in C-rate, DOD and temperature, due to second-order effects that are not captured by the model.

Finally, batteries in the automotive industry often use positive electrodes with mixed chemistries (e.g. LMO\NCA for Nissan Leaf or LMO\NMC for Chevrolet Volt) [36]. Experimental data for cells with these particular chemistries is often not publicly available. Equally, the geometry of cells used in EVs varies – e.g. pouch cells are used in Nissan Leaf, prismatic cells are used in Mitsubishi i-MiEV and cylindrical cells are used in Tesla Model S and X [36]. Although the model was not calibrated for these factors on a cell level, equations have been validated against the on-road data for EVs as discussed in Section 3.2.3

2.5 Overview of the parameter space searched

A number of articles have reported experimental results for calendar and cycling ageing. Some of these have also developed or/and parameterised semi-empirical models based on these results. Although studies on LFP chemistry dominate the literature, other chemistries, most notably NMC and its mixture with LMO are also well covered. Table 1 provides an overview of the scope of the reviewed academic publications.

Table 1 Summary of the key publications discussed in this report showing the scope of each article in terms of degradation mechanisms and studied parameters

Cathode chemistry [anode=graphite unless specified]	Calendar life		Cycle life				Paper reference
	T	SOC	T	DOD	C-Rate	General mechanism	
LFP	x						[7]
LFP	x	x	x	x	x		[8]
LFP	x	x					[9]
LFP	x	x					[13]
LFP			x	x	x		[16]
LFP			x	x	x		[18]
LFP					x		[23]
LFP, LMO, NMC (LTO anode)						x	[2]
LFP, LMO, NMC, NCA						x	[37]
NCA					x		[21]
NCA			x	x			[38]
NMC	x	x	x	x			[10]
NMC			x				[19]
NMC/LMO	x	x	x	x	x		[39]
NMC/LMO	x		x	x	x		[40]
NMC, NCA						x	[6]

2.6 Approach to modelling the effect of managed charging and grid services on battery degradation

EVs can interact with the electricity grid on a few levels as shown in Table 2. The table presents the basic characteristics and parameters in terms of how often the response is required/provided, what type of incentive or price signal is provided (i.e. Time of Use tariffs or direct payments), what reliability of response is expected and whether they do or do not change with time. It also differentiates between integration through charging managed through time of use (ToU) tariffs (typically through the electricity supplier) and integration through the provision of grid services. In practice, grid services are a form of managed charging for EVs, the difference being in the contractual route and the level of automation. Grid services refer to balancing mechanisms National Grid contracts to generators or large users (generally through aggregators for the latter), such as frequency control, Short Term Operating Reserve, etc.

Table 2 EV system integration levels

<table>
<tr><th rowspan="2">Category</th><th colspan="2">User-managed charging</th><th colspan="2">Supplier-managed charging - grid services</th></tr>
<tr><th>Static</th><th>Dynamic</th><th>Grid to Vehicle (G2V)</th><th>Vehicle to Grid (V2G)</th></tr>
<tr><td>Frequency</td><td colspan="2">daily/always</td><td colspan="2">on demand, generally with requested minimum availability windows</td></tr>
<tr><td>Payment</td><td colspan="2">reduced electricity bill</td><td colspan="2">direct payments or reduced electricity bill</td></tr>
<tr><td>New contract in place?</td><td colspan="2">No, usual relationship with electricity supplier (and/or via OEM app)</td><td colspan="2">Contract with aggregator that in turn has a contract with National Grid (or a DNO) or no contract seen by end user e.g. interface with car OEM or electricity supplier only</td></tr>
<tr><td rowspan="2">Implementation options</td><td>Static Time of Use tariffs</td><td>Dynamic Time of Use tariffs</td><td colspan="2">Dynamic Direct Control, with EV owners having control over windows of time offered[4]</td></tr>
<tr><td colspan="2">Indirect management (i.e. user free to respond or not to price signals)</td><td>Control time, duration and/or charge rate</td><td>As Grid to Vehicle plus power from battery is fed back to the grid</td></tr>
</table>

2.6.1 Managed charging

Managed charging and Grid to Vehicle (G2V) interactions do not increase the number of cycles but can alter the battery usage profile primarily by:

a) affecting the average state of charge (SOC);
b) increasing the frequency of charging/discharging events (at equal Ah throughput, more stop/start of the charging or discharging);
c) changing the rate of charge/discharge.

The effect of SOC on calendar ageing is discussed in Section 2.3.2 and is explicitly included in the model. Managed charging strategies have the potential to either increase or decrease the average SOC. Assuming the average battery SOC increases from 50% to 90%, it would result in ca. half the shelf life at typical conditions as discussed in Section 2.3.2. On the other hand, no evidence in the literature was found to support the assumption that the frequency of charging (that does not change the total energy throughput) can affect the battery degradation rate. Consulted battery experts (Dukosi) confirmed that a battery is designed to stop/start charging (this is in effect what happens while driving) and that neither the controls nor the cells are affected by this.

An increase in charge/discharge rate was found to affect the battery degradation as detailed in Section 2.4.1. The model developed as a part of Deliverable 3.2 allows the user to change the rate of charging/discharging. However, the effect of C-rate was found to be relatively minor: switching from 3.3 kW charging to 50 kW charging could cause ca. 5% decrease in the lifetime of a battery (detailed in Section 3.2.1) and therefore the effect may not be prominent in the case of managed charging.

[4] Although National Grid controls the window of time for grid services, it is expected EV users will be given the option by aggregators to opt out on certain day/times. It will be for the aggregators to manage their ability to respond to National Grid demands, e.g. through enrolment of a large number of EVs and incentives for EV owners to participate in managed charging.

An analysis of a few typical cases of managed charging strategies has been conducted assuming a long-range PHEV with the parameters described in Table 3. The aim of this exercise is not to provide an exhaustive list of all possible scenarios for managed charging, but rather to show examples of possible managed charging strategies and their impact on a PHEV battery lifetime. In Stage 2 of the CVEI project, the in-use data obtained from the trial will be used in the SOH model to study the effects of managed charging on battery lifetime and to quantify the associated economic effects.

Table 3 Model inputs for testing different scenarios for managed charging and providing ancillary grid services by a long-range PHEV

Input parameter	Value	Unit
Start date	01/09/2016	
Battery cathode chemistry	NMC	
Total battery pack capacity	16.5	kWh
Battery pack voltage	355	V
Ambient temperature profile	London[5]	
Average C-rate during driving	1	
Average SOC over total capacity	70	%
Charging power (outside of V2G service)	7	kW
Travel profile[6]	User-defined (100 km/day)	
Percentage of travel in full electric mode	70	%
Battery usage in EV mode	0.16	kWh/km
Battery usage in charge sustain mode	0.005	kWh/km

Managed charging is likely to result in delayed charging, i.e. charging does not start immediately after the vehicle is plugged-in. This would decrease the average SOC and lead to extended battery life as demonstrated by Case 1 in Table 4. However, managed charging has also a potential to increase the average SOC, e.g. if the EV users change their behaviour in response to managed charging and plug in the EV earlier than normal. If the charging begins immediately after the vehicle is plugged in, the average SOC can increase as assumed in Case 2 in Table 4. This could have a noticeable effect on the battery lifetime and the user would need to be 'compensated' for this additional degradation, as shown in Table 4. Equally, managed charging can lead to an increase in the charging rate, which may also decrease the battery lifetime, as demonstrated by Case 3 in Table 4. However, if the battery lifetime is not decreased below 12 years, no penalty is assumed in the model. This reflects the fact that 12 years is the average lifetime of a light duty vehicle in the UK, as inferred from the data available from the Department for Transport (DfT). Finally, Case 4 represents a scenario where both the SOC and C-rate increase due to managed charging. Annual compensation of £60-94 would be required in this case depending on the base year for the battery costs. Battery pack costs for 2015 and 2020 base years developed by Element Energy under D3.1 were used (assuming the base case scenario) [41].

[5] Met Office monthly temperatures for London in 2015 (monthly average max: 23.7°C, monthly average min: 8.0°C).
[6] A typical mileage (can be changed in the model) will depend on the EV usage and will be refined in stage 2

Table 4 Summary of the case studies for managed charging

Input parameter	Baseline	Case 1	Case 2	Case 3	Case 4
Relative increase/decrease in SOC (%)	-	-10	10	0	10
Average SOC (%)	70	63	77	70	77
Relative increase in charging rate (%)	-	300	0	300	300
Average C-rate during charging	0.42	1.7	0.42	1.7	1.7
Years until SOH reaches 80% (years)	13.0	13.5	12.0	12.5	11.5
Required annual payment to "break even" (£/year) – based on 2015 battery pack cost	N/A	-	64	0	94
Required annual payment to "break even" (£/year) – based on 2020 battery pack cost	N/A	-	41	0	60

2.6.2 Vehicle to Grid

Vehicle to Grid (V2G) services were found to have a potential to significantly impact battery lifetime through the increased number of cycles. Thus, the model includes the functionality to quantify the additional battery degradation costs due to ancillary grid services. The additional degradation is estimated by the model and additional costs for EV users are then calculated by combining these results with the battery cost projections. Typical grid service values (i.e. those received by the asset or aggregator providing the service) can then be compared with potential cost to EV users from additional battery degradation.

The impact of ancillary grid services on battery degradation have been analysed using several case studies. The model input parameters used for all cases are the same as the ones used for analysing the managed charging strategies and are summarised in Table 3. Under these conditions, the battery is estimated to have a lifetime of 13 years if no grid services are provided. Based on the National Grid's current contracted services, EVs that provide grid services must be available to charge or discharge for a specified amount of time per year ('holding service'), and will actually be charged or discharged during a lesser amount of time. Only the actual use has an impact on battery and therefore only this use is modelled. EVs are assumed to constantly charge/discharge within the specified DOD during the time that they are providing the V2G service in the model. Although, in reality the charging/discharging may be distributed across the service holding time with periods of no activity in-between, this distribution does not affect degradation provided that the throughput is the same.

Two types of ancillary grid services are considered in the model – a) firm frequency response and b) balancing services. Firm frequency response is an automatic change in active power output or demand in response to a frequency change. Services are procured through a competitive tender process, where tenders can be for low frequency events, high frequency events, or both [42]. The balancing mechanism type service in the UK is STOR (Short term operating reserve). This service requires the provision of extra power through standby generation, and/or demand reduction, in order to be able to balance unforeseen mismatches in supply and demand [42].

Holding payments of £11-20/MW/hour are available for dynamic Firm Frequency Response (FFR) based on National Grid accepted tender data [43]. Typical FFR utilisation is from 1.4% to 6.9% depending on the response characteristics. 6.9% assumes that the battery starts responding at a deviation of 0.05 Hz and delivers full response at a deviation of 0.2 Hz. This is based on analysis of per-second resolution frequency data provided by National Grid [44]. Availability payments for STOR are typically £3/MW/hr and utilisation payments are £100-150/MWh based on the most recent National Grid reports [45]. This service is procured for Mon - Fri 07:00 - 13:30, 16:00 - 21:00 and Sat - Sun 10:30 - 13:30, 16:00 - 20:30 and is typically called on 70 times per year for 2 hours each time (meaning that utilisation time is limited to ca. 3% of total holding time).

In line with the battery degradation analysis, the following parameters were found to affect battery lifetime in the case of V2G service provision:

a) charge/discharge power (kW) at which the service is provided;
b) DOD range utilised for the service;
c) Percentage of holding time that the service is utilised (held at 3% in all cases in Table 5).

Specific cases that have been analysed to estimate the impact of V2G services are summarised in Table 5. The DOD window was limited to 5% in Cases 1 and 3 to represent FRR service which is likely to require the battery to charge and discharge within a narrow range. The entire useable capacity of the battery (90% DOD) is available for the services in cases 2 and 4 to reflect STOR requirements. In scenarios where services were modelled assuming domestic charging capability (cases 1 and 2), the impact on battery life was insignificant both when DOD was limited to 5% of the total PHEV battery capacity as well as when the entire useable capacity of the battery (90% DOD) was utilised. This is due to a very low number of added equivalent full cycles. However, when the services are provided at high power (Cases 3 and 4), the number of cycles due to service provision increases significantly and leads to much higher degradation. The lifetime decrease is particularly high in Case 4 because of intensive cycling at 90% DOD. Note that the battery degradation proceeds at accelerated rate when the DOD is higher than at 5% as discussed in Section 2.4.3. In-depth analysis of the likelihood of various strategies for the EV integration into the grid is outside of the scope of this Stage 1 report. However, the data collected during the CVEI Stage 2 trial will provide the opportunity to inform managed charging and V2G scenarios. Based on the observed response to demand management, the SOH model and wider analytical framework will be used to determine the impact of demand management on battery life and inform strategies to minimise this impact.

Table 5 Summary of the case studies for providing V2G grid services

Input parameter	Baseline	Case 1	Case 2	Case 3	Case 4
Type of service	None	FFR	STOR	FFR	STOR
Power available (kW)	-	3	3	50	50
DOD window for service (% of total capacity)	None	5	90	5	90
Holding time (hr/day)	None	8	8	8	8
Utilisation time (hr/day)	None	0.2	0.2	0.2	0.2
Years until SOH reaches 80% (years)	13.0	13.0	12.8	11.2	8.0
Added equivalent full cycles per year (for services)	N/A	16	19	265	447
Required annual payment to “break even” (£/year) – based on **2015** battery pack cost	N/A	0	0	118	462
Required annual payment to “break even” (£/year) – based on **2020** battery pack cost	N/A	0	0	76	295
Estimated value of the service provided (£/year)	N/A	96	53	1,488	876

For the purpose of this preliminary economic assessment the incremental annualised battery replacement cost was estimated for the cases presented in Table 5 using battery pack costs for 2015 and 2020 base years developed by Element Energy under D3.1 [41]. The results show that services provided at high power (50 kW) lead to substantial decrease in battery lifetime and would require a compensation of £462/year (based on 2015 battery pack cost) assuming Case 4 from Table 5. For reference, analysis of current grid service revenues shows almost twice higher value, assuming the holding and utilisation assumptions used in Case 4 [43]–[45]. The case of providing Firm Frequency response at high power (Case 3) results in even higher revenues because the service holding value is higher. This suggests that the revenues received for providing grid services would be sufficient to compensate EV owners for the costs of providing V2G services at high power. Although conclusions

on the feasibility of grid services cannot be made based on the limited number of analysed cases presented here, the SOH tool can be used for more in-depth analysis.

V2G services in Cases 1 and 2 cause relatively small degradation (or even no additional degradation in Case 1) because only a small number of equivalent full cycles is added due to service provision.

In conclusion, the following should be considered in order to lessen the economic impact of V2G services:

- Power limitation to ensure that the battery is not extensively cycled during provision of grid services;
- DOD limitation to ensure that the battery degradation proceeds at a lower rate – note that the model includes three DOD windows and the rate of degradation is different in each band;
- The choice of positive electrode chemistry and ensuring that the pack is not overheating as high temperatures were found to accelerate degradation

2.7 Summary of the modelling approach

The inputs of the battery SOH model can be categorised into (a) battery properties, (b) travel data, (c) charging data and (d) price forecasts. Battery properties determine the coefficients and scaling factors that the model uses. Travel data is a proxy for vehicle usage profiles. The average values are defined for some of the parameters affecting battery lifetime to reproduce different degradation pathways. The charging data is combined with the travel data to account for the effect of high charging rates, additional cycles due to V2G services, etc. Price forecasts for grid services and battery replacement are used to calculate the revenue generated from providing grid services. This is shown schematically in Figure 8.

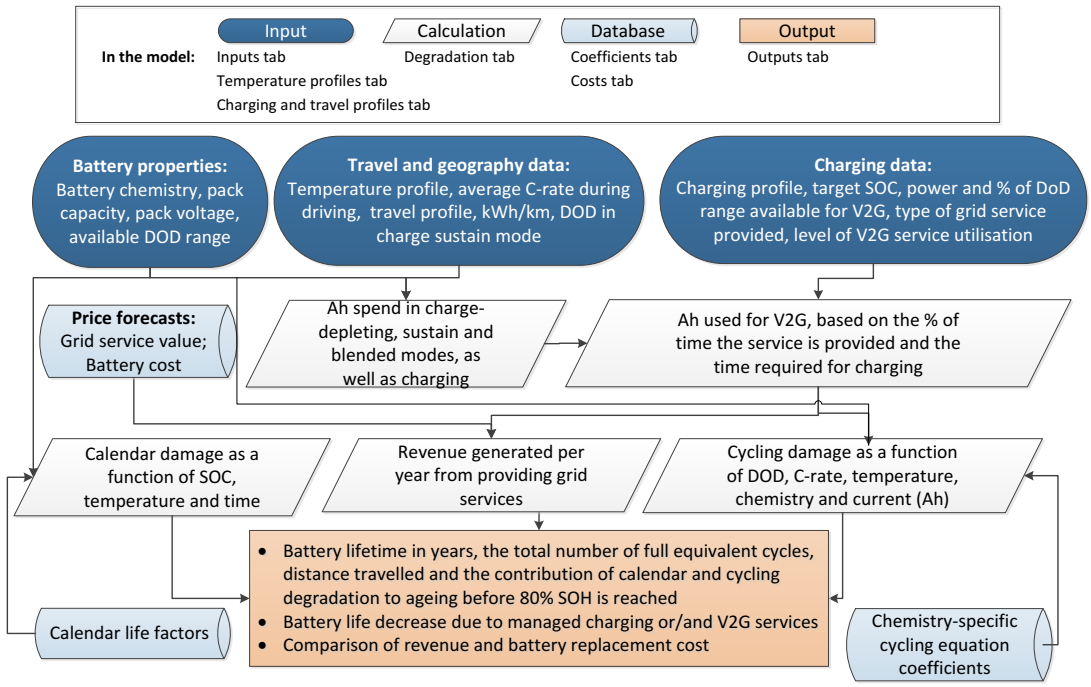

Figure 8 Schematic of the SOH model showing input categories, data flow, and outputs

The useable battery pack capacity is used in the model to calculate the number of full equivalent cycles based on the total current throughput. The available DOD window in EVs is limited by manufacturers to reduce safety risks and maximise the battery life. This is schematically represented in Figure 9. Although the DOD window varies with the battery chemistry and level of thermal management in place,

a typical allowed DOD window is 85% for BEV packs and 70% for PHEV packs. Note that in the model the DOD window is limited from the top only for simplicity (i.e. the maximum SOC is 85%).

The model calculates cycling ageing by combining total current throughput (Ah) in (a) charge depleting[7], (b) charge sustaining[8], (c) blended[9], (d) slow charging (3.3 or 7 kW), (e) rapid charging (22, 43, 50 or 150 kW) and (f) V2G service modes. It is important to account for the throughput in each of these modes separately as DOD and C-Rate can be different, e.g. shallow cycling (0-5% DOD) is likely to be used during the charge sustain mode and deep cycling may be relevant for the charge depleting mode in PHEVs. Calendar and cycling ageing is assumed to be the same for all standard chemistries (LFP, NMC, and NCA). Cycling damage is combined with calendar damage to calculate battery lifetime in years and the number of full equivalent cycles before the end-of-life (80% SOH) is reached. All of the parameters that the model is not parametrised for (e.g. electrolyte) are assumed to have the same effect on degradation in all cases.

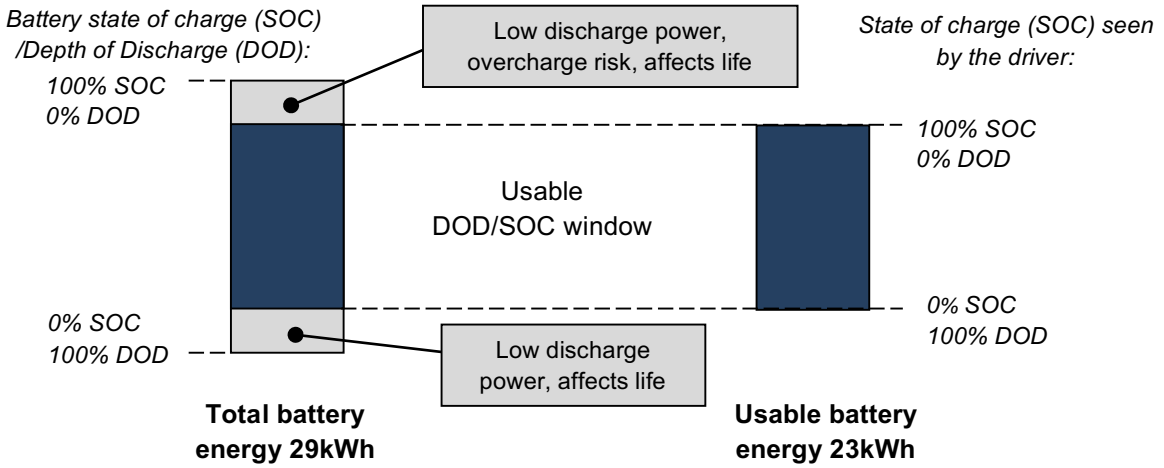

Figure 9 Useable versus nominal battery capacity illustration, adapted from [46]

An example of the key model outputs is shown in Figure 10; capacity fade due to calendar ageing and cycling ageing are distinguished. The model also estimates the contribution of V2G service provision to the decrease in battery lifetime. V2G services have the potential to decrease the lifetime of battery mainly through additional battery cycles. However, if a high C-Rate and/or a deep DOD are used for providing V2G services, this may further decrease the lifetime by affecting the average C-rate and DOD values.

Additionally, managed charging may have an effect on C-Rate if the charging rate is slowed down or made higher, e.g. to provide frequency regulation. The potential contribution of this is relatively small, but it is nevertheless considered in the model. The contribution would be small because the C-rate cannot be much higher than the starting C-rate, if at all (limited by the charging point and vehicle on-board charger). For example, when charging at home at 3 or 7 kW, the charging point will not cope/allow a higher rate. Furthermore, it is unlikely distribution network operators would encourage higher power rates. Therefore, if charging is managed through a change of C-rate, it is more likely to be through lower charging rates.

Note that the potentially more frequent battery on/off switching for V2G services is not expected to affect the lifetime. Frequency of battery cycling is not linked to any of the key ageing parameters detailed

[7] PHEV mode in which power is provided exclusively from the battery. BEVs always operate in this mode.
[8] PHEV mode in which the battery is used to optimise the engine performance by discharging during power peaks at high RPMs and charging from the engine during low RPMs. HEVs always operate in this mode.
[9] PHEV mode in which power is provided both by the engine and the battery. The battery is partly recharged by the engine or regenerative braking during driving.

before (temperature, DOD, C-rate, SOC). In summary, the model developed under WP3 outputs the following key parameters:

- Battery lifetime (year when 80% SOH of total capacity is reached)
- Total number of full equivalent cycles
- Number of full equivalent cycles annually
- Annual revenue assuming the selected grid service value
- Annual revenue required to "break even"
- Distance travelled in charge-depleting mode
- Distance travelled in charge-sustaining mode
- Total distance travelled

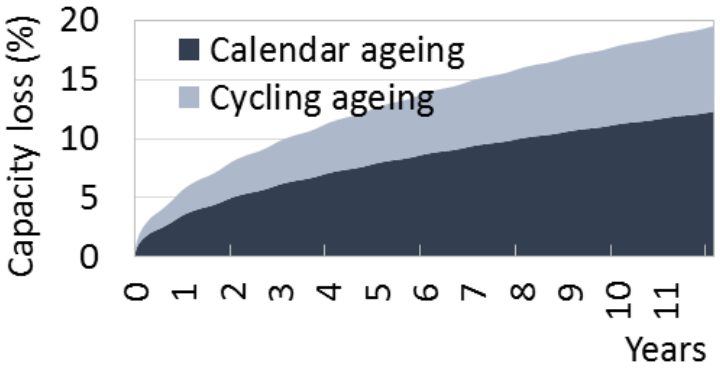

Figure 10 Example of the model output demonstrating accumulated calendar and cycling damage

The developed model is intended to provide a sufficiently accurate battery lifetime prediction in order to estimate the feasibility of managed charging and Vehicle to Grid services. On the other hand, the model cannot be used to develop new battery chemistries and is not intended to provide sufficient accuracy to be applied to real-time SOH calculations on-board a vehicle.

Battery degradation is a complex combination of multiple processes and the battery research community did not yet succeed to explain all the processes involved. Thus, algorithms that model battery degradation need to have some embedded assumptions. Table 6 summarises the assumptions used for the SOH model developed as a part of this project. Assumptions represent the current prevalent view in the scientific community (e.g. calendar ageing is caused by the loss of Li inventory) and reflect the sometimes limited availability of data.

Table 6 The summary of assumptions used for the model development

Assumption	Comment
Calendar degradation occurs due to Li corrosion at the SEI layer causing the loss of Li inventory.	Clear consensus in the scientific community. However, this is an approximation and other mechanisms may be contributing to calendar ageing. Data on other parameters and their impact is not available.
Calendar ageing is governed by the processes on the interface between the electrolyte and the negative electrode.	Clear consensus in the scientific community. The choice of positive electrode may also have a minor effect on calendar ageing, which is not captured.
The degradation rate depends on the absolute DOD window for the cycle, but not on the central SOC for this cycle.	Any potential interdependencies between the SOC and DOD are not captured. The reviewed literature does not investigate these potential interdependencies and all the publications reviewed used the same average SOC.
The same degradation mechanisms are valid for the entire modelled range of all parameters e.g. same equations applied to low and high temperatures.	Some degradation modes may not be captured. Data is not available for the full range of the possible parameters, e.g. no published research shows systematic degradation test results for very low temperatures.
The results of static experiments can be used to model dynamic profiles maintaining the accuracy sufficient for the purpose of this work.	A loss in modelling accuracy is to be expected for highly dynamic usage profiles. No data available to investigate the potential variation in degradation rates when varying several parameters; in published research, typically a single parameter is varied.
The data from cell manufacturer datasheets (at standard conditions: room temperature, 100% DOD) can be used to derive the coefficient that models the effect of the positive electrode chemistry on degradation (used in the cycling ageing equation). The same degradation equation applies across positive electrode chemistries (only one coefficient varies).	The derived coefficients might have been different if calibrated outside of standard conditions. This means the modelled variation across positive electrode chemistries is not validated by data for cases where the temperature and DOD are not standard, nor is the equation used. No comparable data across a set of conditions is available for different chemistries. Although the methodology observed across publications varies, there is evidence that the same form of equation is applied to various Li-ion chemistries.
The effect of parameters for which the model could not be parametrised, such as cell size, format, electrolyte type, electrode thickness, specific electrode blends and temperature gradients in the battery pack can be ignored for the purpose of this work.	The result of the model provides only an estimate of the degradation. The same assumptions are made in academic publications using semi-empirical equations for modelling battery degradation. The SOH model uses the same parameters (temperature, SOC, DOD window, time, C-rate) than in the literature.

3 Statistical analysis of EV battery degradation and model result validation with EV real world data

3.1 Surveys of EV drivers

New BEVs and PHEVs are sold with a warranty covering the battery pack from the manufacturer. This gives a broad indication on how long the battery manufacturer expects the battery to last in real-life conditions. At the same time, until recently most manufacturers did not offer any capacity warranty for their battery packs. Notably, Nissan has recently amended their battery warranty to cover capacity – it states that all Leafs will maintain a charge of at least 70% of original capacity for the first 5 years/60,000 miles (ca. 100 000 km) [47], [48]. Capacity retention is of particular importance for BEV buyers, as this is directly linked to the driving range. However, even the leading EV models have been on the market for less than 10 years. Therefore, only limited actual data on battery pack degradation in real-life conditions is available. In the absence of robust systematic testing data, statistics gathered from EV owners may be used as a guide for estimating battery capacity fade. The requirement for higher measurement precision in smaller PHEV battery packs make it more difficult to extract valuable data from these user surveys and hence this section focuses on BEVs.

LFP batteries are widely used in automotive applications by Chinese manufacturers. Automobile manufacturer BYD based in Shenzhen, China, launched its first all-electric e6 sedan in 2010. In 2013, the company announced that 30 EV taxis operating in Shenzhen travelled 400 000 km on average and have a capacity fade of less than 9% [49]. The claimed e6 range of 300 km implies approximately 1 300 battery cycles after 400 000 km. The degradation calibrated with BYD data for individual LFP cells in Figure 6 is indeed just below 9% after 1 300 cycles. However, direct comparisons should be made with caution since 1 300 full cycles take less than 4 months in the laboratory environment. BYD's announcement suggests that single-cell degradation in steady-state laboratory conditions can be extended to real-life operation under dynamic load conditions in a battery pack without any modifications. This information should be treated as indicative only, as neither provided details on how the capacity loss was estimated, nor were the results assessed by an independent party.

A survey of 240 owners of Nissan Leafs fitted with a 24 kWh (21.3 kWh usable) battery pack with LMO\NCA cathode suggested less than 15% capacity loss after ca. 20 000 km driven [50]. The drawback of this survey is that owners of the EVs were asked to report how many capacity bars are displayed on the EV control panel at full charge. The absence of one or more bars would indicate a capacity loss. Over 90% of the drivers reported that their cars are still showing all capacity bars at the time of the survey, suggesting that the capacity loss is anywhere between 0% and 15% (refer to Section 3.2 for more results on the Nissan Leaf). More interestingly, the survey results indicated that most of the drivers who did report capacity loss after ca. 20 000 km were using cars in a hot climate. The Nissan Leaf has a passive thermal management system, so climatic conditions may affect the battery operating temperature both during driving and when parked outside. This reiterates the importance of including temperature into the ageing equations.

A similar study by "Plug In America" surveyed 234 Tesla Roadsters by contacting owners through Tesla Motors Club and collecting data through Open Vehicle Motoring System [47]. The results suggested 0.15% capacity loss per 1 000 miles, which translates into ca. 3.8% capacity loss after 40 000 km, the average distance travelled by the EVs surveyed. Using these results to forecast further degradation would assume that the rate of degradation is constant throughout battery lifetime. However, this is not likely to be the case as was demonstrated by another Tesla Model S survey. As shown in Figure 11, degradation of the 85 kWh battery pack with an NCA cathode levels off after ca. 50 000 km at 5%. This behaviour is in line with square root dependency on time for calendar ageing and almost square root dependency on current throughput for cycling ageing. On the other hand, surveys of Tesla EVs did not reveal any discernible patterns for degradation dependency on climate. Active liquid cooling installed on Tesla battery packs goes some way towards explaining this.

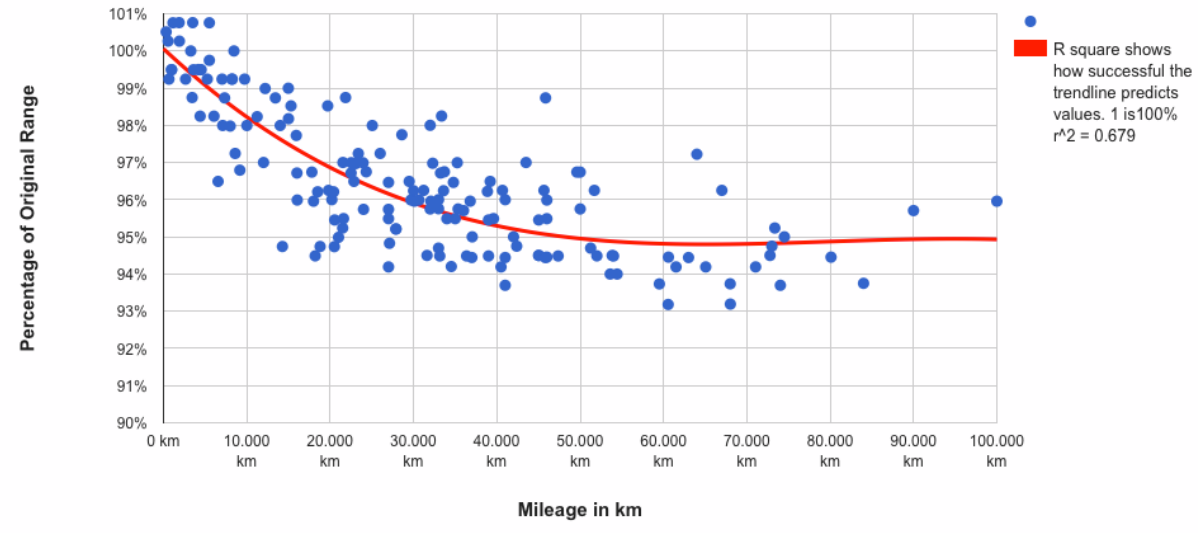

Figure 11 Capacity loss estimation for 85 kWh battery pack with NCA cathode in 80 Tesla Model S vehicles obtained through European Tesla Motors Club and showing slowdown in degradation after ca. 50 000 km travelled [51]

In conclusion, the results of surveys have a large statistical spread and should be used for sense checking, rather than for validation. These surveys are not directly comparable, but suggest some common trends:

- Degradation reported in surveys is moderate (less than 10%) even after substantial travelled distances (>100 000 km).
- Degradation rate is not constant and is likely to decrease with time.
- Battery pack design has an effect on degradation, e.g. through the choice of cooling system.

3.2 Battery testing results for on-road BEVs and PHEVs

Systematic EV battery testing in laboratory conditions is necessary to provide insights into battery degradation needed for reliable model validation. Idaho National Laboratory (INL) conducts battery testing for on-road EVs on a regular basis. These experiments are conducted based on a testing procedure developed by the United States Advanced Battery Consortium and the results are publically accessible on INL's website [52]. INL publishes on-road usage and a performance summary along with the battery degradation for each vehicle. This information has been used to validate the results of the model.

3.2.1 BEV testing

Idaho National Laboratory has published laboratory battery testing results for several Nissan Leaf S cars (2013) operated over a fixed on-road duty cycle [52]. All of the vehicles were exposed to similar conditions, summarised in Table 7. The variations in each value between the vehicles is also shown in Table 7. Battery capacity loss was analysed at INL by performing Static Capacity Tests and the Electric Vehicle Pulse Power Characterization Tests.

Results for 3 Nissan Leafs (2013) are shown along with the modelled degradation in Figure 12. Although the travelled distance is similar for all vehicles, two of the vehicles have been driven for 450 days, while VIN 0646 has been driven for 618 days. The testing of all three vehicles started around the end of January 2014. Although the average SOC is not reported for the vehicles the on-road usage statistics published by INL show a statistical distribution of SOC before and after charging events. The SOC was reported to be above 50% more than 70% of the time when the vehicles were plugged in. Also, the vehicles were charged to above 90% SOC around 90% of the time according to the statistics provided. The SOC is treated as an uncertainty for modelling, but it is expected that models assuming a high SOC

(>50%) should yield better correlation with the observed degradation. The modelled results are shown for two different cases – SOC = 80% and SOC = 20% in Figure 12.

Table 7 Extract of key on-road usage, performance and battery pack degradation data for Nissan Leaf S (2013) available on the INL website [52]

Parameter	Value	Variation (+/-)
Overall electrical energy consumption (kWh/km)	0.18	0.02
Percent of city travel	90%	8%
Charging power (kW)	7	1
Average ambient temperature (°C)	32[10]	1

For the purpose of modelling calendar degradation, it was assumed that BEVs were driving 20 000 km in a year. Calendar and cycling ageing were combined in the model and a custom chemistry coefficient (0.195)[11] was used. The modelling results for SOC = 80% agree better with the final observed degradation. Degradation rate decreases around 15 000 km due to colder ambient temperature, as this corresponds to late autumn and winter. The degradation rate picks up again around 25 000 km as the temperature rises in April.

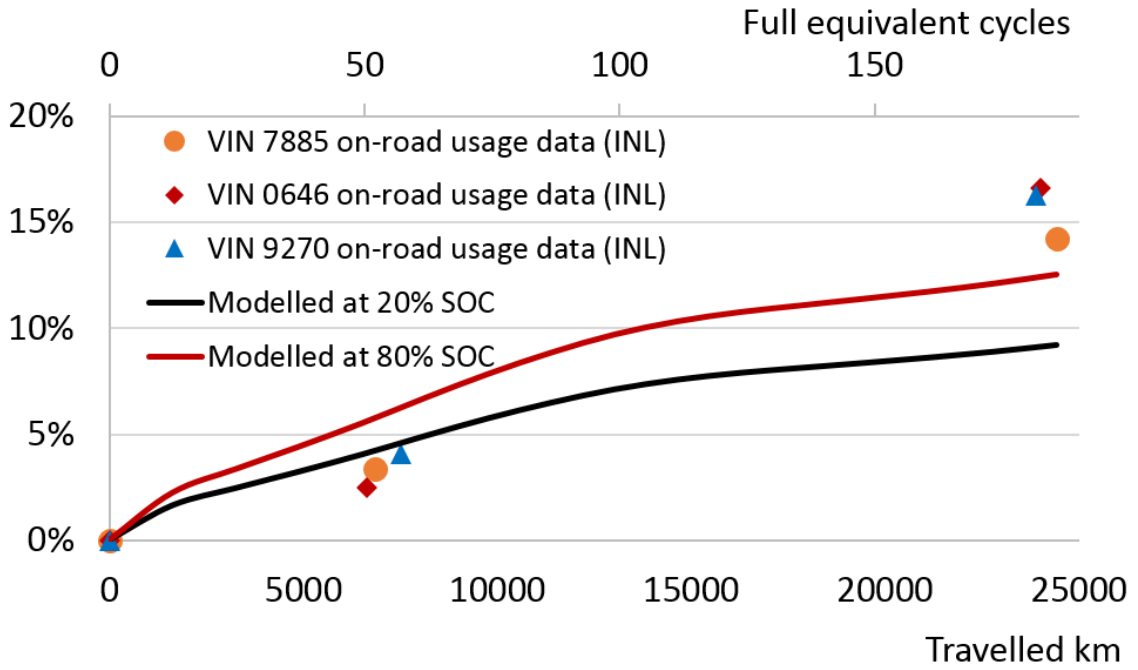

Figure 12 Battery degradation for 3 different on-road Nissan Leaf S (2013) reported by Idaho National laboratory and the model results for the same conditions

Whilst the modelled results show deviation from the actual degradation, it is important to note that the observed degradation for different vehicles also shows a degree of spread in values. VIN 7885 has degraded by 14.2% and VIN 9270 by 16.3% within the same timeframe, despite being exposed to identical conditions. This emphasises the fact that even the batteries from the same manufacturer

[10] INL collected the CAN signal for ambient temperature only then the vehicle was operation (i.e. during driving). As this ignores the times of the day when the vehicle is parked, notably the nigh-time temperatures, the average Phoenix, Arizona, USA temperature profile has been used for modelling instead [55].

[11] Nissan Leaf uses LMO-NCA cathodes in its batteries. Direct calibration of the model for this type of cathode is not possible as Nissan does not provide any experimental degradation curves for its batteries. Therefore, the customs coefficient has been adjusted so that the resulting degradation matches the actual data as closely as possible whilst also keeping all other testing parameters in line with the data on testing conditions (e.g. temperature, kWh/km).

exposed to identical conditions may degrade differently (likely as a result of minor differences in manufacturing and operating conditions).

The effect of rapid charging on battery degradation was reported by the INL for the Nissan Leaf (2012) [53]. Two vehicles were charged exclusively at 3.3 kW, while the other two vehicles were fast charged at 50 kW. All vehicles were operated over a fixed on-road duty cycle and were charged twice a day for 1.5 years. Average driving energy consumption over the duration of the project was ca 0.14 kWh/km for all vehicles. The battery pack temperature that was taken at the beginning of each charge and at the beginning of duty cycle was between 15 °C and 40 °C, with the median value of 32 °C. It was concluded that residual heat from rapid charging elevates the pack temperature slightly for the next drive, but the change is relatively minor (ca. 1.5-2 °C).

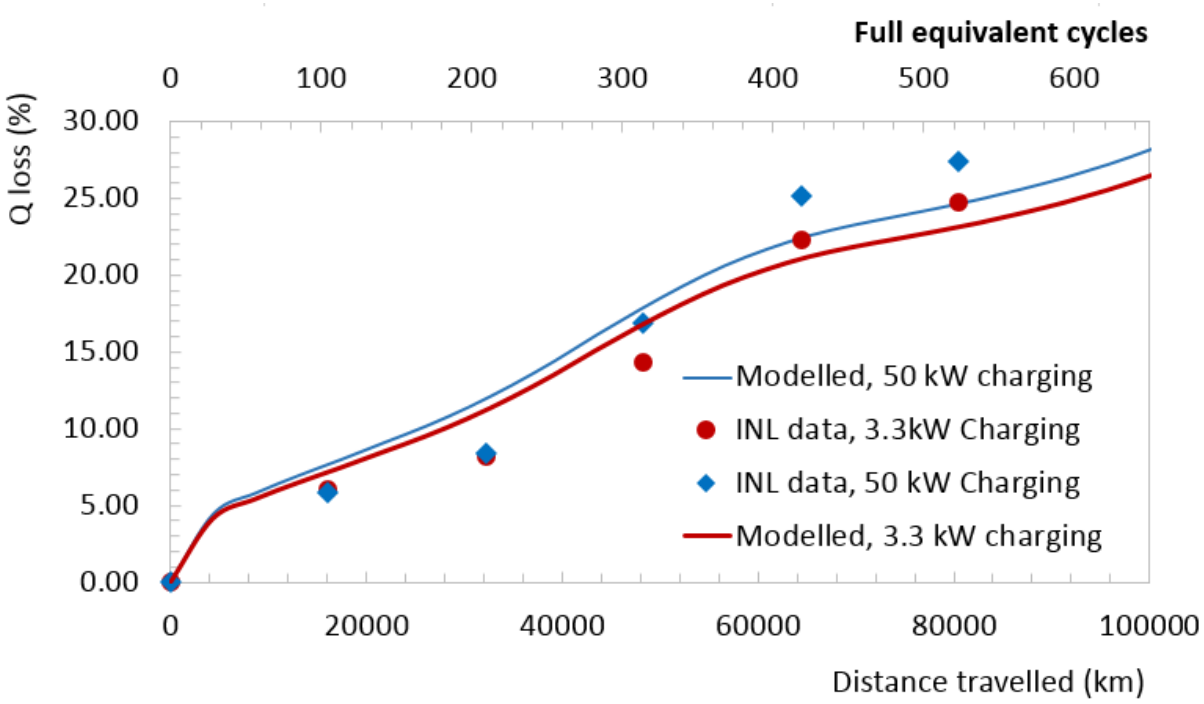

Figure 13 Comparison of the modelled and INL data [53] for battery capacity loss for vehicles using slow and rapid charging

The testing started in November 2014 and continued for 15 months. The traction battery packs were removed and tested when the vehicles were new, and at 16 100 km (10,000 miles) intervals. The battery tests showed that while the fast charged vehicles did lose more capacity than the control vehicles, the difference was small relative to the total capacity loss, as shown in Figure 13. The overall capacity loss at the end of the experiment was ca. 25%, with less than 3% points attributable to the effect of rapid charging. It should be noted that this could have been indirectly caused by rapid charging through the increase in battery pack temperature during charging, in addition to the direct effect of the higher C-rate.

The modelling results shown in Figure 13 assume a SOC = 80% and demonstrate a relatively good agreement with the actual data. The decrease in the degradation rate between 40 000 km and 80 000 km is due to lower ambient temperatures during the winter period (November to March). Note that the observed degradation after the first 25 000 km in Figure 12 is ca. 15%, whilst the degradation in Figure 13 is under 10%. In both cases the vehicles were driven in the same climate, were exposed to similar duty cycles and charging routines. Partly the difference is explained by the fact that the results in Figure 12 are shown for the vehicles that travelled 25 000 km in approximately a year, whilst the results in Figure 13 are for vehicles that travelled the same distance in less than 5 months. Therefore, the calendar damage in Figure 13 is somewhat lower than in Figure 12 for the same travelled distance. However, modelling results suggest that the effect cannot be fully explained by the difference in

calendar ageing. As previously noted, this underlines the complex nature of battery ageing and the challenge of model parameterisation.

3.2.2 PHEV testing

Battery packs in PHEVs are smaller compared to BEV packs in terms of capacity and are on average exposed to milder (low DOD) cycling conditions. The INL published results on battery capacity tests for several PHEV models on their website [52]. Figure 14 compares the modelled results with the actual data for the plug-in Toyota Prius (2013). This PHEV model has a 4.4 kWh battery pack with an NCA cathode and air cooling [54]. For modelling purposes, the temperature profile for Phoenix, Arizona, USA was assumed [55]. Three Toyota Priuses (2013) were driven ca. 50% of the total travelled distance in urban environments and 50% on the highway and charged at 7 kW. The tests started in July 2013 and lasted two and a half years until the end of 2015. The test vehicles were travelling ca. 90 000 km per year.

The INL data does not provide information on the SOC for PHEVs. The INL on-road usage statistics for Toyota Prius (2013) suggests that around 70% of all trips were in charge sustain mode, with the rest being in a blended mode (trips where fuel was consumed by the engine, and net electrical energy was consumed from the battery to propel the vehicle). Typically, the EV would switch to charge-sustain mode when the SOC is relatively low. With the majority of trips in charge sustain mode, it is reasonable to assume low SOC on average for the purpose of modelling. The SOC has been varied in the model to get the best correlation with the actual data. The modelling results at 15% SOC show a good match with the actual data (Figure 14). No trips in full electric mode are assumed in this case, in line with INL data.

An EV in charge sustain mode uses only a small DOD window (5% has been assumed in the model), which puts cycling ageing into the bin with the lower degradation rate (0-5%). Energy flow during the charge-sustain mode is not normally measured and reported, therefore an estimate of 0.005 kWh/km has been assumed[12]. It should be noted that this captures both the discharge and charge during driving, as the battery is never depleted.

Similar analysis has been conducted on several Chevrolet Volt (2013) with a 16.5 kWh LMO\NMC battery that was tested for 3 years starting in January 2013 in similar conditions (Phoenix, Arizona in the United States) temperature profile; 90 000 km/year; 7 kW charging). The main difference with the Toyota Prius testing was that the Chevrolet Volt drove 13% of the total distance in full electric mode, according to INL data. The results are shown in Figure 15. Degradation that is modelled assuming the average SOC = 15% is in a good agreement with the measured capacity loss. The variations in degradation rate in Figure 14 and Figure 15 (manifesting itself as changes in curvature) are due to variations in temperatures throughout the year in both experiments (the vehicles were tested during a 3-year period in both cases).

Although the degradation observed for the Toyota Prius (Figure 14) and the Chevrolet Volt (Figure 15) are similar (reaching ca. 10% after 200 000 km in both cases), the reasons for degradation are slightly different. In the case of the Toyota Prius, the cycling damage is relatively low because of operation exclusively in charge-sustain mode and calendar ageing dominates the degradation.[13] The Chevrolet Volt has a larger battery and 13% of the total travelled distance is driven in full EV mode, which results

[12] There are no directly useable data on this in the literature. INL reports 0.02 kWh/km for Prius in a blended-mode (Trips where gasoline was consumed by the engine, and net electrical energy was consumed from the battery to propel the vehicle). However, in a charge-sustaining mode, the net energy consumption is -0.003 kWh/km. This number does not indicate what the throughput is (which is what is needed here), because the battery could have been cycled a lot in charge-sustain mode without taking any net energy from it. Trial data will provide (confirmation from TRL is pending – actual as of 31/01/2017) the information on which mode of operation was used in conjunction with high-resolution SOC in-use data, which can then be used to derive energy throughput, see the Annex for more information on how the Phase 2 managed charging trial data will be used.

[13] Note that separation into calendar and cycling ageing is available in the model but not shown in Figure 14 and Figure 15 for clarity.

in the increased rate of cycling degradation. On the other hand, the trial of the Chevrolet Volt started in winter and the temperature in the first few months of operation was relatively low leading to a lower initial rate of calendar degradation, which has offset a higher cycling degradation. The dashed line in Figure 15 shows the modelled degradation that would have occurred if the trial had started in July (same as the trial for Toyota Prius).

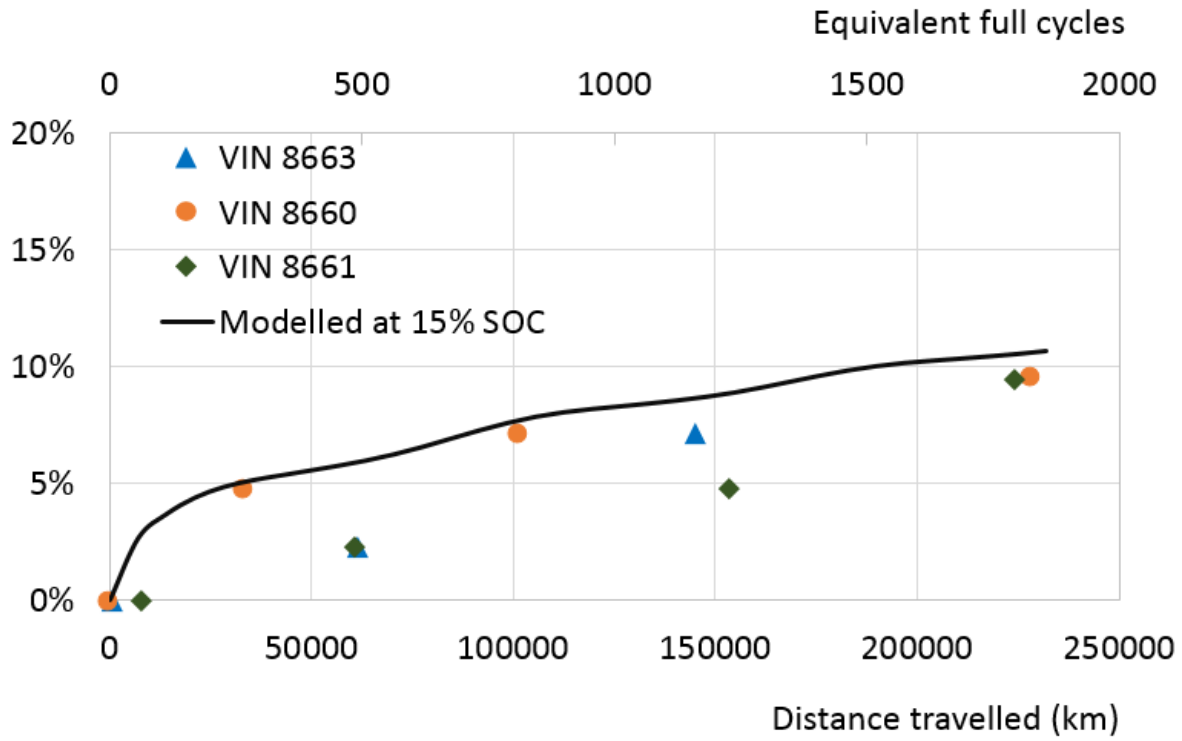

Figure 14 Battery degradation for 3 different on-road Toyota Prius (2013) reported by Idaho National laboratory and the model results for the same conditions for SOC = 15%

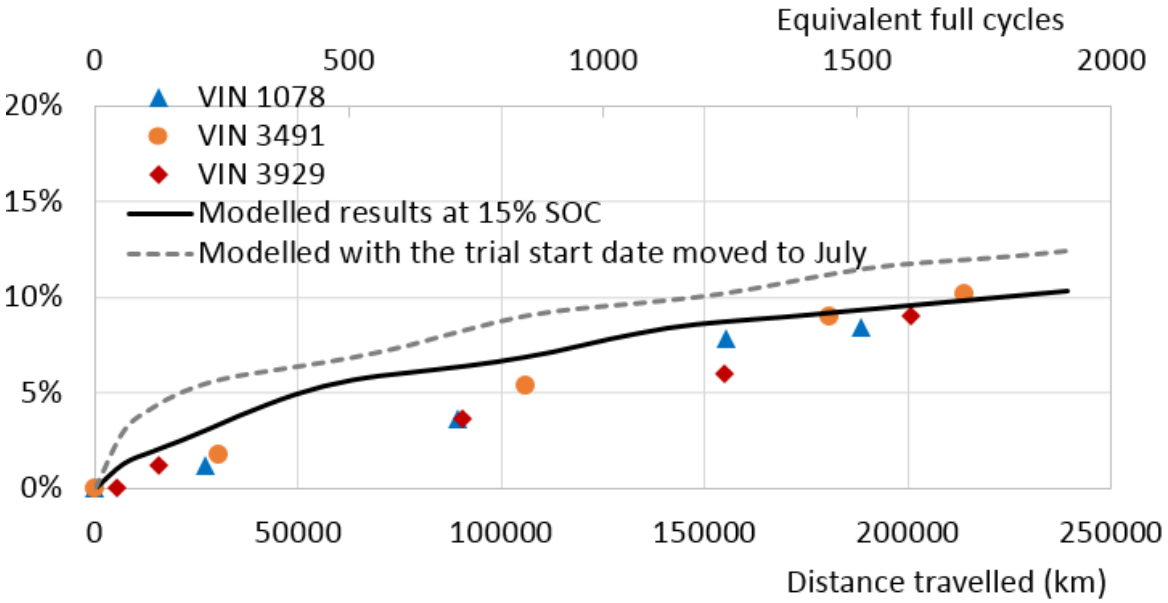

Figure 15 Battery degradation for 3 different on-road Chevrolet Volt (2013) reported by Idaho National laboratory and the model results for the same conditions for SOC = 15%

4 Summary and conclusions

4.1 State of health modelling

The model has been developed and calibrated using the latest available data from the following sources: (a) academic publications; (b) OEM data sheets; (c) EV testing report and (d) EV owner surveys. The primary ageing mechanisms and the sensitivity to certain parameters, e.g. DOD or C-rate, was found to vary between the sources. This is due to the complexity of the underlying battery ageing mechanisms, which are still not fully understood. Analysis of the academic literature has been conducted in parallel with consultations with automotive battery industry experts in order to develop the model algorithm that reflects battery ageing trends. To satisfy the requirement for the model to use simple inputs (i.e. measurable on-board a vehicle), a semi-empirical modelling approach has been chosen. The model inputs were disaggregated into the following categories: (a) battery properties, e.g. capacity; (b) travel and geography data, e.g. temperature and (c) charging data, e.g. charging power. The battery degradation was separated into the calendar ageing and cycling ageing components. While the former increases with time, the latter increases with the current throughput (Ah). The following general relationship has been developed and parameterised to account for the total capacity loss:

$$Q_{loss} = f(T, Chemistry, DOD, SOC, C_{rate}, Ah, t)$$

The majority of the reviewed sources were found to agree on the effect of temperature, SOC, current throughput and time, on battery degradation. The effect of DOD and C-rate is less studied in literature but generally, batteries are reported to degrade faster when cycled at high DOD and high C-rate. These findings are reflected in the model.

The review has covered all of the lithium-ion chemistries currently used in EVs[14]. The degradation of LFP batteries was found to be well documented, while an increasing number of recent publications was found to cover NMC and LMO batteries (refer to Table 1). At the same time, the data for NCA batteries (used by Tesla) remains relatively scarce. The analysis of the underlying degradation mechanisms indicated that battery chemistry is likely to have an effect on ageing. Chemistry-specific coefficients were calibrated for LFP, NMC and NCA batteries using manufacturers' technical spreadsheets. It should be noted that degradation rates were found to vary even between batteries with same chemistries and therefore the model additionally allows the user to specify a custom chemistry-specific factor.

The battery degradation rate was found to follow broadly a square root relationship with time and current throughput (Ah). Elevated temperatures were found to be a major contributor to both calendar and cycling ageing. High SOC was found to increase calendar ageing, while a high C-rate was found to accelerate cycling ageing. However, the effect of C-rate during rapid charging (50 kW) was found to be relatively minor (refer to Figure 13).

The model has been successfully validated against both cell level testing under laboratory conditions and pack level testing under on-road conditions. Comparing the modelling results with the measured data from various sources showed that a certain variation in battery degradation, which is not captured by the model, should be expected. This is due to the complexity of the underlying phenomena that the model aims to replicate. However, all of the observed EV battery ageing trends are correctly reflected in the model and may be used to estimate battery lifetime in typical operating conditions.

4.2 Summary of potential economic and technical impact of demand management and V2G strategies

Potential effects of managed charging and ancillary grid services on battery lifetime have been analysed in Section 2.6. It was concluded that while potential changes in SOC during managed charging can

[14] Note that some EV manufacturers use blended or otherwise modified cathode chemistries, which are typically protected by intellectual property rights. These have not been explicitly covered in this report.

noticeably impact battery lifetime, charge/discharge power and the DOD window will determine the impact of V2G services on battery degradation. Equally, the increase in C-rate both during managed charging and V2G services may cause additional cycling damage, although this was shown not to be significant. A function to quantify the decrease in battery lifetime due to ancillary grid services has been included in the model.

EV battery pack costs are used in the model for the economic assessment of managed charging and V2G service provision. Managed charging that does not significantly increase the average SOC was found to require only minor additional payments to EV owners. If the SOC is decreased by introducing managed charging, the EV battery lifetime may even increase, providing an additional incentive for EV owners to participate in managed charging.

Preliminary analysis revealed that V2G services at high power (50 kW) can result in noticeable additional degradation, particularly if the DOD window available for the service is not limited. Scenarios where V2G services were provided limiting the EV charge/discharge power to 3 kW, causes only a minor increase in battery cycling and hence did not lead to a significant decrease in battery lifetime. The services provided at low power and low DOD may be a good entry point for a V2G service rollout. The developed modelling tool can be used to conduct a comprehensive analysis of various possible charging and grid service scenarios by varying relevant inputs.

4.3 Research and data gaps

The SOH model was developed for lithium-ion batteries, the technology that currently dominates the EV market. The calendar and cycling ageing equations have been calibrated with data for batteries with LFP cathodes, as this type of battery is best represented in the academic literature. Batteries with blended cathodes (e.g. LMO\NMC) are increasingly used in automotive industry, but there is a lack of systematic studies on the degradation of such cells in academic literature. Therefore, the model has been calibrated with the experimental data for batteries with NMC and NCA cathodes at standard conditions, available from battery manufacturers, and a custom chemistry coefficient was used to validate the results for the blended cathode chemistry of the Nissan Leaf (Figure 12 and Figure 13). However, it is recognised that batteries with different cathodes may respond slightly differently to changes in C-rate and DOD. The review of available literature has also shown that the degradation rate may vary by manufacturer even for identical chemistries (detailed in Section 2.4.5).

In the 2020s or later, new technologies might enter the automotive market, such as lithium metal (e.g. lithium sulphur) batteries. The anode in lithium-ion batteries is also expected to transition from graphite to a blend of graphite and silicon [41]. In both cases, one impediment to the rollout of these technologies is that the cycle life is currently too short for automotive applications. As such, there is not yet systematic data on parameters affecting lifetimes of these batteries, as there is for the battery chemistries that have been included in this SOH model. It is therefore not possible to comment on the impact of demand management or V2G provision on such future batteries.

The developed model can be used for a first order assessment of the impact of managed charging strategies. However, inherent limitations of the semi-empirical approach do not allow the entire range of factors that may affect battery lifetime to be captured in this model. Fundamental research of degradation mechanisms in Li-ion batteries combined with a systematic experimental analysis of these mechanisms is required and will lead to improved accuracy of State of Health models. A lack of understanding of the fundamental degradation mechanisms in Li-ion batteries has been emphasised by industry experts and further research and testing has been outlined as the key to advance State of Health modelling.

5 References

[1] G. K. Prasad and C. D. Rahn, "Model based identification of aging parameters in lithium ion batteries," *J. Power Sources*, vol. 232, pp. 79–85, 2013.

[2] X. Han, M. Ouyang, L. Lu, J. Li, Y. Zheng, and Z. Li, "A comparative study of commercial lithium ion battery cycle life in electrical vehicle: Aging mechanism identification," *J. Power Sources*, vol. 251, pp. 38–54, 2014.

[3] A. Barré, B. Deguilhem, S. Grolleau, M. Gérard, F. Suard, and D. Riu, "A review on lithium-ion battery ageing mechanisms and estimations for automotive applications," *J. Power Sources*, vol. 241, pp. 680–689, 2013.

[4] B. Scrosati and J. Garche, "Lithium batteries: Status, prospects and future," *J. Power Sources*, vol. 195, no. 9, pp. 2419–2430, 2010.

[5] M. Broussely, S. Herreyre, P. Biensan, P. Kasztejna, K. Nechev, and R. J. Staniewicz, "Aging mechanism in Li ion cells and calendar life predictions," *J. Power Sources*, vol. 97–98, pp. 13–21, 2001.

[6] M. Kerlau, M. Marcinek, V. Srinivasan, and R. M. Kostecki, "Studies of local degradation phenomena in composite cathodes for lithium-ion batteries," *Electrochim. Acta*, vol. 53, no. 3 SPEC. ISS., pp. 1386–1393, 2007.

[7] M. Koltypin, D. Aurbach, L. Nazar, and B. Ellis, "More on the performance of LiFePO4 electrodes-The effect of synthesis route, solution composition, aging, and temperature," *J. Power Sources*, vol. 174, no. 2, pp. 1241–1250, 2007.

[8] E. Sarasketa-Zabala, E. Martinez-Laserna, M. Berecibar, I. Gandiaga, L. M. Rodriguez-Martinez, and I. Villarreal, "Realistic lifetime prediction approach for Li-ion batteries," *Appl. Energy*, vol. 162, pp. 839–852, 2016.

[9] E. Sarasketa-Zabala, I. Gandiaga, E. Martinez-Laserna, L. M. Rodriguez-Martinez, and I. Villarreal, "Calendar ageing analysis of a LiFePO4 graphite cell with dynamic model validations: Towards realistic lifetime predictions," *J. Power Sources*, vol. 275, pp. 573–587, 2015.

[10] M. Ecker, N. Nieto, S. Kaebitz, J. Schmalstieg, H. Blanke, A. Warnecke, and D. U. Sauer, "Calendar and cycle life study of Li(NiMnCo)O2-based 18650 lithium-ion batteries," *J. Power Sources*, vol. 248, pp. 839–851, 2014.

[11] A. Hackbarth, B. Lunz, R. Madlener, D. U. Sauer, and R. W. de Doncker, "Plug-in Hybrid Electric Vehicles for-CO2 Free Mobility and Active Storage Systems for the Grid (Part 2)," *E.ON Energy Res. Cent. Ser.*, vol. 2, no. 3, 2010.

[12] A. Hackbarth, B. Lunz, R. Madlener, D. U. Sauer, and R. W. de Doncker, "Plug-in Hybrid Electric Vehicles for CO2-Free Mobility and Active Storage Systems for the Grid (Part 1)," vol. 2, no. 3, 2010.

[13] M. Kassem, J. Bernard, R. Revel, S. Pélissier, F. Duclaud, and C. Delacourt, "Calendar aging of a graphite/LiFePO 4 cell," *J. Power Sources*, vol. 208, pp. 296–305, 2012.

[14] S. Grolleau, A. Delaille, H. Gualous, P. Gyan, R. Revel, J. Bernard, E. Redondo-Iglesias, and J. Peter, "Calendar aging of commercial graphite/LiFePO4 cell - Predicting capacity fade under time dependent storage conditions," *J. Power Sources*, vol. 255, pp. 450–458, 2014.

[15] M. Dubarry, C. Truchot, and B. Y. Liaw, "Synthesize battery degradation modes via a diagnostic and prognostic model," *J. Power Sources*, vol. 219, pp. 204–216, 2012.

[16] J. Wang, P. Liu, J. Hicks-Garner, E. Sherman, S. Soukiazian, M. Verbrugge, H. Tataria, J. Musser, and P. Finamore, "Cycle-life model for graphite-LiFePO4 cells," *J. Power Sources*, vol. 196, no. 8, pp. 3942–3948, 2011.

[17] I. Bloom, B. W. Cole, J. J. Sohn, S. A. Jones, E. G. Polzin, V. S. Battaglia, G. L. Henriksen, C. Motloch, R. Richardson, T. Unkelhaeuser, D. Ingersoll, and H. L. Case, "An accelerated calendar and cycle life study of Li-ion cells," *J. Power Sources*, vol. 101, no. 2, pp. 238–247, 2001.

[18] E. Sarasketa-Zabala, I. Gandiaga, E. Martinez-Laserna, L. M. Rodriguez-Martinez, and I.

Villarreal, “Cycle ageing analysis of a LiFePO4/graphite cell with dynamic model validations: Towards realistic lifetime predictions,” *J. Power Sources*, vol. 275, pp. 573–587, 2015.

[19] Y. J. Lee, H. Y. Choi, C. W. Ha, J. H. Yu, M. J. Hwang, C. H. Doh, and J. H. Choi, “Cycle life modeling and the capacity fading mechanisms in a graphite/LiNi0.6Co0.2Mn0.2O2 cell,” *J. Appl. Electrochem.*, vol. 45, no. 5, pp. 419–426, 2015.

[20] J. D. K. Bishop, C. J. Axon, D. Bonilla, M. Tran, D. Banister, and M. D. McCulloch, “Evaluating the impact of V2G services on the degradation of batteries in PHEV and EV,” *Appl. Energy*, vol. 111, pp. 206–218, 2013.

[21] D. Wong, B. Shrestha, D. A. Wetz, and J. M. Heinzel, “Impact of high rate discharge on the aging of lithium nickel cobalt aluminum oxide batteries,” *J. Power Sources*, vol. 280, pp. 363–372, 2015.

[22] Idaho National Laboratory, “Effects of Electric Vehicle Fast Charging on Battery Life and Vehicle Performance,” 2015.

[23] J. Groot, M. Swierczynski, A. I. Stan, and S. K. Kær, “On the complex ageing characteristics of high-power LiFePO4/graphite battery cells cycled with high charge and discharge currents,” *J. Power Sources*, vol. 286, pp. 475–487, 2015.

[24] M. Ben-marzouk, A. Chaumond, E. Redondo-iglesias, M. Montaru, and S. Pélissier, “Experimental protocols and first results of calendar and / or cycling aging study of lithium - ion batteries – the MOBICUS project,” pp. 1–10, 2016.

[25] N. Omar, M. A. Monem, Y. Firouz, J. Salminen, J. Smekens, O. Hegazy, H. Gaulous, G. Mulder, P. Van den Bossche, T. Coosemans, and others, “Lithium iron phosphate based battery–Assessment of the aging parameters and development of cycle life model,” *Appl. Energy*, vol. 113, pp. 1575–1585, 2014.

[26] G. Suri and S. Onori, “A control-oriented cycle-life model for hybrid electric vehicle lithium-ion batteries,” *Energy*, vol. 96, pp. 644–653, 2016.

[27] T. Qiu, J. Wang, Y. Lu, and W. Yang, “Improved elevated temperature performance of commercial LiMn2O4 coated with LiNi0.5Mn1.5O4,” *Electrochim. Acta*, vol. 147, pp. 626–635, 2014.

[28] S. B. Chikkannanavar, D. M. Bernardi, and L. Liu, “A review of blended cathode materials for use in Li-ion batteries,” *J. Power Sources*, vol. 248, pp. 91–100, 2014.

[29] BYD, “Build your dreams - LFP Battery Info,” 2014.

[30] Kokam, “KBM series module,” 2016.

[31] Joerg Kuempers (Johnson Controls Saft Advanced Power Solutions GmbH), “Neue Fahrzeugkonzepte mit dem Fokus Nachhaltigkeit : Lithium- Ionen Batterien für Elektrofahrzeuge,” 2010.

[32] M. Berecibar, I. Gandiaga, I. Villarreal, N. Omar, J. Van Mierlo, and P. Van Den Bossche, “Critical review of state of health estimation methods of Li-ion batteries for real applications,” *Renew. Sustain. Energy Rev.*, vol. 56, pp. 572–587, 2016.

[33] A123 Systems, “Cycle Life Testing: The Lithium Ion Battery Ultramarathon.” [Online]. Available: http://www.a123systems.com/Cycle-Life-Testing-The-Lithium-Ion-Battery-Ultramarathon.htm.

[34] Valence, “Valence’s Lithium Iron Magnesium Phosphate Battery has a long cycle life,” 2016. [Online]. Available: https://www.valence.com/why-valence/long-lifecycle/. [Accessed: 14-Apr-2016].

[35] K2 Energy, “High capacity LFP26650EV Energy cell data.” .

[36] M. Anderman, “xEV Battery Technology Status and Advances,” no. January, 2015.

[37] H. Popp, J. Attia, F. Delcorso, and A. Trifonova, “Lifetime analysis of four different lithium ion batteries for (plug–in) electric vehicle,” *Transp. Res. Arena*, 2014.

[38] S. Watanabe, M. Kinoshita, T. Hosokawa, and K. Morigaki, “Capacity fading of LiAlyNi1-x-y CoxO2 cathode for lithium-ion batteries during accelerated calendar and cycle life tests,” *J.*

Power Sources, vol. 260, pp. 50–56, 2014.

[39] M. Ben-Marzouk, A. Chaumond, E. Redondo-iglesias, M. Montaru, and S. Pélissier, "Experimental protocols and first results of calendar and / or cycling aging study of lithium - ion batteries – the MOBICUS project," *EVS29 Symp.*, pp. 1–10, 2016.

[40] J. Wang, J. Purewal, P. Liu, J. Hicks-Garner, S. Soukazian, E. Sherman, A. Sorenson, L. Vu, H. Tataria, and M. W. Verbrugge, "Degradation of lithium ion batteries employing graphite negatives and nickelecobaltemanganese oxide þ spinel manganese oxide positives: Part 1, aging mechanisms and life estimation," vol. 269, pp. 937–948, 2014.

[41] Element Energy for ETI, "Deliverable D3.1: Battery Cost and Performance and Battery Management System Capability Report and Battery Database," 2016.

[42] Element Energy for University of Durham, "Customer-Led Network Revolution Part1: Review of existing commercial arrangements and emerging best practice," 2013.

[43] National Grid, "Services Reports." [Online]. Available: http://www2.nationalgrid.com/UK/Industry-information/Electricity-transmission-operational-data/Report-explorer/Services-Reports/. [Accessed: 22-Apr-2016].

[44] National Grid, "Enhanced Frequency Response." [Online]. Available: http://www2.nationalgrid.com/Enhanced-Frequency-Response.aspx. [Accessed: 22-Apr-2016].

[45] National Grid, "Market Information & Tender Round Results." [Online]. Available: http://www2.nationalgrid.com/UK/Services/Balancing-services/Reserve-services/Short-Term-Operating-Reserve/Short-Term-Operating-Reserve-Information/. [Accessed: 22-Apr-2016].

[46] Element Energy for The Committee on Climate Change, "Cost and performance of EV batteries," 2012.

[47] T. Saxton, "Plug In America's Tesla Roadster Battery Study," pp. 1–14, 2013.

[48] InsideEVs, "Nissan Makes Good On Battery Warranty Pledge For 2011-2012 LEAF Owners," 2012. [Online]. Available: http://insideevs.com/nissan-leaf-battery-swap-under-warranty-video/. [Accessed: 25-Apr-2016].

[49] Wuzhou city, "BYD Electric Vehicle Fleets: A Centerpiece in the Celebration of a Wuzhou's New Green Chapter," *04/11/2013*. [Online]. Available: http://www.byd.com/news/news-182.html. [Accessed: 31-Mar-2016].

[50] T. Saxton, "Plug In America's LEAF Battery Survey," pp. 1–12, 2012.

[51] J. Jivan, "Tesla Model S battery degradation shown to level off at 5% after 30,000 miles," *08/05/2015*, 2015. [Online]. Available: http://electrek.co/2015/05/08/tesla-model-s-battery-degradation-shown-to-level-off-at-5-after-30000-miles/. [Accessed: 31-Mar-2016].

[52] Idaho National Laboratory, "Advanced Vehicle Testing Activity." [Online]. Available: https://avt.inl.gov/content/pubs-az. [Accessed: 15-Apr-2016].

[53] M. Shirk and J. Wishart, "Effects of Electric Vehicle Fast Charging on Battery Life and Vehicle Performance," 2014.

[54] Navigant Research, "The Lithium Ion Battery Market," 2014.

[55] U.S. climate data, "Climate Phoenix - Arizona," 2015. [Online]. Available: http://www.usclimatedata.com/climate/phoenix/arizona/united-states/usaz0166. [Accessed: 28-Sep-2016].

6 Annex – Use of CVEIP Phase 2 trial data in the State of Health Model

The Phase 2 managed charging trial will generate a dataset that can be used in the Excel State of Health (SOH) model to calculate the capacity loss of an EV battery under different driving and charging conditions. The processing required in order to use the trial data in the SOH model is described here, to demonstrate that the model will be able to make full use of the data following updates in Phase 2. The annex covers the following aspects:

- the trial data resolution;
- the proposed resolution and 'dynamism' in the Phase 2 SOH analysis;
- the trial outputs required for the SOH model;
- the trial data processing for the use in the SOH model.

The trial data resolution and the background for processing

The dynamic nature of driving means that the time-step required to capture the variation in key trial parameters is in the order of seconds. Therefore, the trial will generate a journey dataset with key parameters available with 10-second resolution (e.g. SOC during journey) and a charging dataset with key parameters (e.g. SOC during charging) available with 5-minute resolution.[15] Using higher resolution sub-minute data in the SOH model is not beneficial in terms of accuracy for the chosen method of the SOH estimation (semi-empirical approach) as discussed below. Equally, handling the data with a sub-minute resolution is impractical in Excel as the data will exceed the spreadsheet row limit. Given that the proposed 5-minute resolution in the SOH model for Phase 2 can be accommodated within the current Excel-based model, we do not propose to change the modelling platform for Stage 2.

The journey data will be converted to a 5-minute resolution in order to combine it with the charging data available at this resolution. Equations used in the SOH model have a certain degree of non-linearity, which can lead to accuracy loss when input data is averaged. Figure 16 and Figure 17 compare the effect of converting data with 10-second resolution to 5-minute and 1-day resolution for a hypothetical case. In this example, an EV with a 24 kWh battery pack is assumed to make two journeys every day, each journey lasting one hour. The energy throughput during each journey is randomly generated within a pre-defined limit of 0.12 kWh/km and 0.25 kWh/km. The EV is then assumed to fully charge at night at 7 kW to the target SOC of 80%. The temperature is assumed to be constant at 10°C for this example. The purpose of this exercise is to understand whether averaging the inputs for the SOH model has a significant impact on accuracy.

The results shown in Figure 16 suggest that the degradation modelled using 5-minute resolution is indistinguishable from the degradation calculated from the original 10-second dataset. As expected, the degradation calculated from data averaged over the entire day, e.g. using only a single value for each parameter, is linear during the day and does not represent the actual degradation throughout the day well. However, the loss in accuracy for the end-of-the-day degradation is relatively small even in that case.

Figure 17 demonstrates that the loss in accuracy is relatively small both in the case of averaging inputs to 5-minute and 24-hour intervals when calculated over a period of one month. The loss in accuracy at the end of the month is only 0.01 percentage point for 5-minute resolution and 0.03 percentage points for 1-day resolution. The reason for this low sensitivity of the results to the resolution of data is that the equations have a low level of non-linearity for key inputs. This does not undermine the requirement for collecting the journey data at 10-second resolution, as this is a prerequisite for being able to average some of the inputs (e.g. C-rate) correctly.

[15] As per information shared by TRL. Confirmation on data logging from VW and EVConnect pending (current as of 31/01/2017).

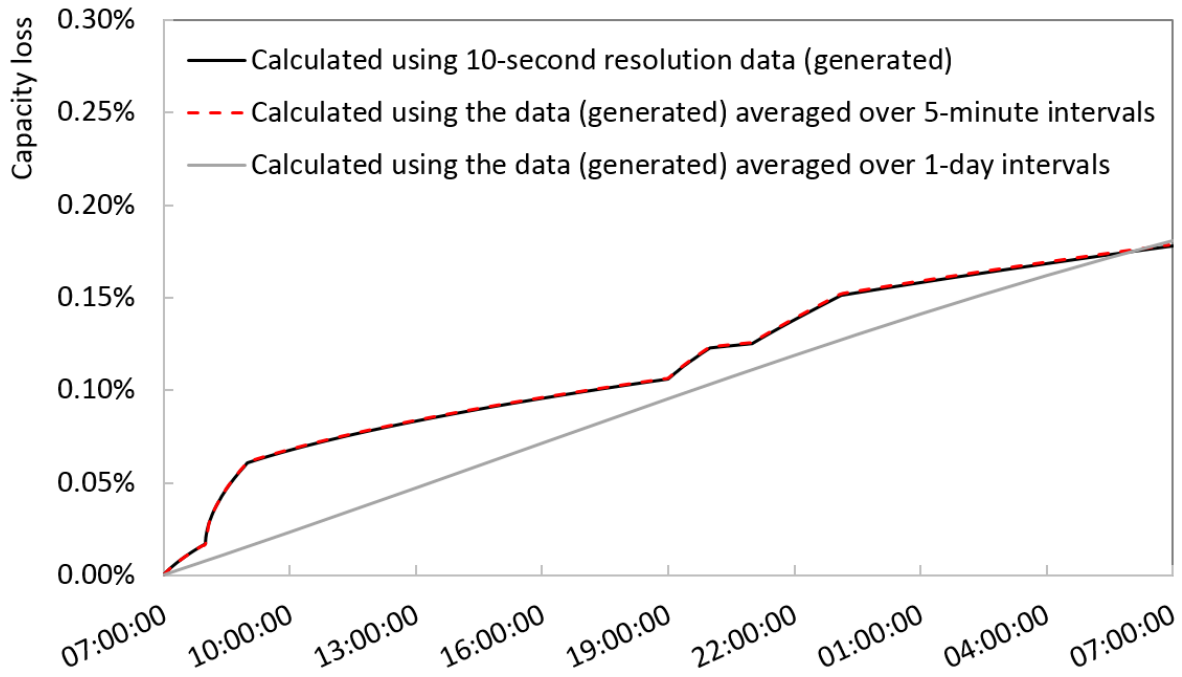

Figure 16 Comparison of battery degradation calculated over a 24 hour period using a hypothetical driving profile

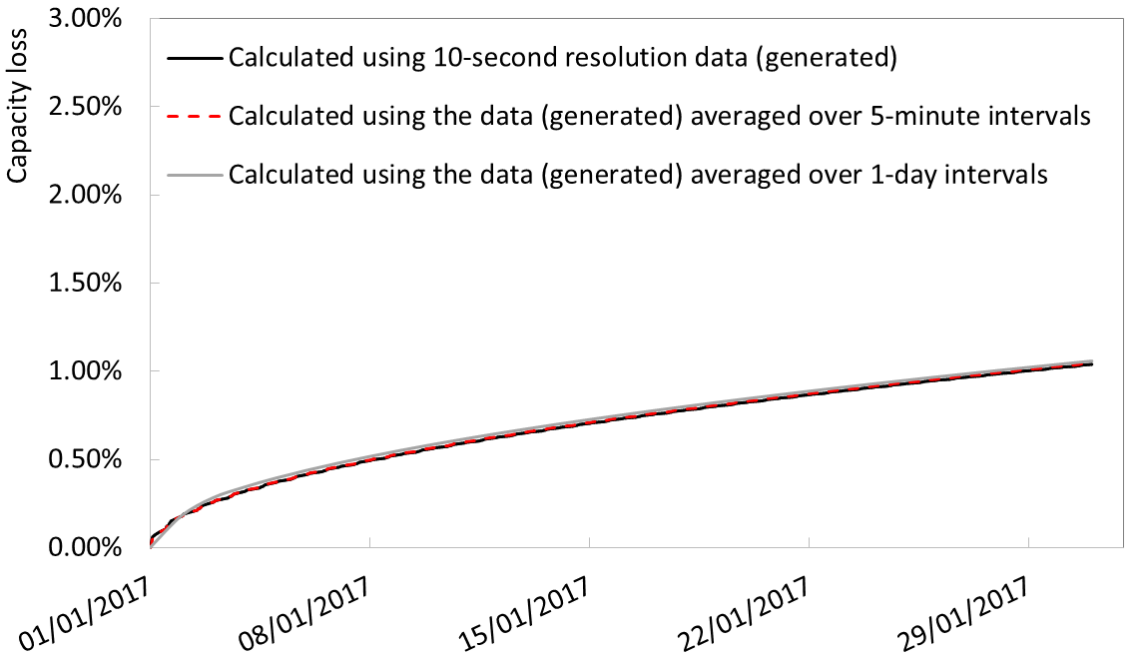

Figure 17 Comparison of battery degradation calculated over a period of one month using a hypothetical driving profile

Modifications to the SOH model in Phase 2

The current SOH model will be modified in Phase 2 in order to make it able to accept the 5-minute data set out above. The capacity loss calculation will be conducted for each 5-minute interval (instead of daily) by changing the resolution of the “Degradation” tab. The underlying equations and coefficients will not be affected. The separation of degradation into calendar and cycling, and into further sub-categories for the case of cycling ageing, will also remain unaffected as the processing of trial data will

ensure that degradation is separated into these categories. All the relevant formulas in the model will be modified to use the actual data from the trial. The model will use unique values for energy flow, C-rate and SOC for each 5-minute interval. This will ensure that the model can fully capture the dynamics inherent in different journey patterns and charging scenarios.

Description of the required trial data

There are numerous parameters that will be recorded during the trial (as of 31/01/2017, confirmation from TRL is pending on the exact list) and that will be required for the SOH model. These are summarised in Table 8 and the comments on how each of the parameters will be used in the SOH model are below.

- The vehicle, participant, trial and journey identification numbers will be used to reconcile the data from different datasets (if necessary) and to create a number of typical travel and charging profiles that will capture the travel and charging patterns for all trial participant groups.
- The odometer reading will be used to plot battery capacity loss versus travel distance.
- The SOC at ignition on/off and the SOC during journey (with 10-second resolution) is the key trial output that will be used in the SOH model. This parameter will be used to calculate the throughput and the C-rate (both used in the cycling ageing equation) during each 10-second interval. The SOC will also be used directly in the equation for calendar ageing.
- The average speed, road class and type will be used in case additional analysis of the results or the construction of counterfactual hypothetical travel profiles is necessary. It is expected that energy consumption will depend on the average speed, road class and type. Therefore, being able to link energy consumption to these variables will allow an analysis of hypothetical travel profiles if required.
- The maximum C-rate will be used to cross-check the C-rate calculated from the energy consumed during the journey. It is expected that the C-rate averaged over a 10-second interval should be a good approximation of the actual C-rate. However, maximum C-rate may need to be used if a vehicle spends significant portion of the 10-second period stationary.
- Time spent stationary will be used to decide on whether to use maximum or average C-rate for the period. This will be the key metric for making the choice between the maximum and the average C-rate. If the stationary time for the period is relatively large, the average C-rate is not a good approximation, so the maximum C-rate will be used. On the other hand, if the stationary time for the period is small, even if there are high peaks in C-rate (e.g. due to acceleration), the average value is likely to be a better approximation for the purposes of calculating the cycling ageing.
- The driving mode will be used to indicate charge depletion, or blended/charge sustaining driving for the case of PHEVs. The actual DOD window used during driving in each of these modes will determine which DOD coefficient will be applied for the period. Since the bands are discrete, a weighted average DOD cannot be used and the throughput in each driving mode will need to be converted into the equivalent throughput using the coefficient for the relevant DOD window. Each DOD window is defined as the difference between the maximum and the minimum SOC during an interrupted operation in a given driving mode. Simple rules will be developed to determine the start and end of one continuous operating mode.
- Plug-in and plug-out date and time will be used to determine when the vehicle is available for Vehicle to Grid (V2G) services. Since vehicles are assumed to be available for V2G only from home, a tag with location (home/away from home) will be derived (by TRL partners) from the GPS data and used in conjunction with the plug-in and plug-out date and time.
- SOC with 5-minute resolution for all charging events will be used to calculate the energy throughput during charging. This will also be used to calculate the C-rate and DOD window for the period.

Table 8 Trial data required for the State of Health modelling[15]

Field	Description	Source
Vehicle ID	Unique reference number for vehicle	RAC
Participant ID	Unique reference number for participant	TRL/Cenex
Trial ID	Uptake Trial or Charging trial	TRL/Cenex
Experimental group	Charging group participants belong to (control / User-managed charging / supplier-managed charging)	TRL/Cenex
Journey ID	Unique reference number for each journey	TRL/Cenex
Odometer reading	Odometer reading at end of journey (i.e. ignition off)	RAC
Average speed (km/h, or mph)	Average speed during 10-second period	RAC
Road type (rural or urban)	Road type used during 10-second period	RAC
Road class (motorway, A road, lower class road)	Road class used during 10-second period	RAC
SoC during journey (including at ignition on and off)	Battery State of Charge (SoC) during 10-second period	RAC
Maximum C-rate	Maximum discharge rate of the battery within 10-second period	RAC
Time spent stationary (s)	Time spent stationary during 10-second period	RAC
Driving mode (PHEV only)	PHEV driving mode currently active (charge depleting, charge sustain or blended)	RAC
Plug in and plug out date and time	Date and time of plug in and plug out	RAC
Charge point location	Home, away from home.	RAC
SOC during charging	Battery State of Charge (SoC) during 5-minute period	EV Connect

Trial data conversion and use in the model

The parameters listed in Table 8 may be part of a single dataset or several datasets (e.g. telematics, charging, etc.). In the latter case, the relevant identification numbers provided with each dataset will be used to aggregate the parameters into a single dataset. A pre-processing routine will derive the following parameters with a 5-minute resolution from the trial data:

- SOC (%) is expected to be available as one of the core trial outputs. It will be used to derive the energy throughput and to group it into driving and charging in each available mode (for driving: charge depleting or blended mode and charge sustain mode; for charging: home, away from home). The grouping into driving modes may be based on the data (listed above) or derived bottom up from the SOC profile. For charging, the input data on charge location will be used to differentiate between home and work charging. Additionally, the C-rate derived from the SOC will be used to identify rapid-charging events. Separate throughput for each mode is required in order to assign it to the correct DOD band when calculating the cycling ageing.

- C-rate – this will be a single weighted average value for all modes in a given 5-minute period (maximum C-rate may be used during journey, based on the time stationary as described above). C-rate is part of the cycling ageing equation.
- DOD will be used to calculate equivalent throughput for each 5-minute period. The equivalent throughput needs to be calculated in order to reflect the difference in cycling ageing rate based on the DOD window.

Conversion between the trial data and the SOH model inputs will be carried out either with a MatLab or an SQL routine. The converted data will then be directly pasted into the Excel SOH model. The data conversion is schematically represented in Figure 18. Note that the full quantity of trial data will be used in the model. For example, data from multiple weeks of operation will be run through the SOH algorithm; we will not create average profiles before entry into the SOH model, since these risk hiding week to week variations. Similarly, data from each individual user will used separately to calculate SOH impacts, as there could be significant differences in usage patterns between users (such as regular use of rapid charging or not). This approach will maximise the model's ability to capture differences between users and different weeks.

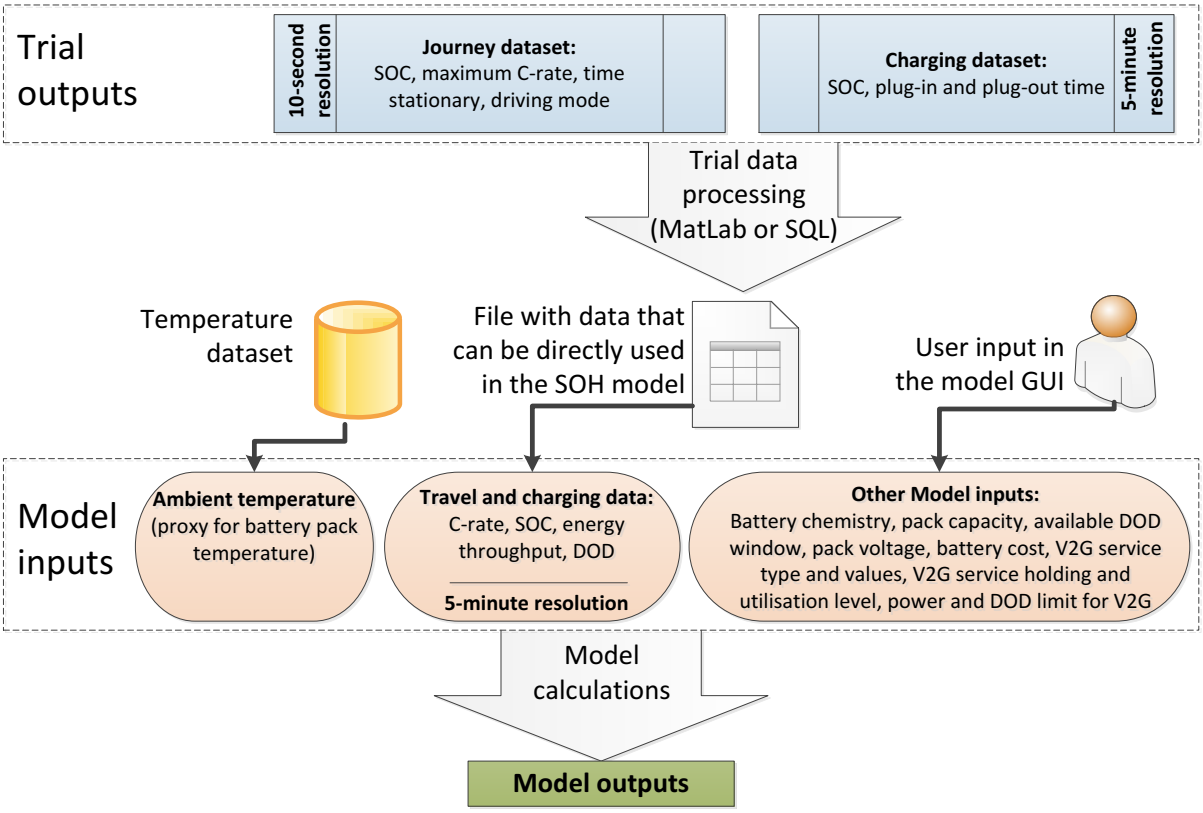

Figure 18 Schematics of the trial data conversion for the use in SOH model

The SOH model aims to forecast battery degradation over the lifetime of an EV and therefore the calculations will need to be extended beyond the timeframe of the trial. This will be achieved by repeating the usage patterns generated during the trial.

Since neither the cell nor the battery pack temperature is expected to be recorded during the trial[15], ambient temperature will be used as a proxy for battery temperature in the SOH model. The dataset of temperatures for the appropriate climate station in the UK (e.g. Heathrow station for London) will be used in the model. The temperature of battery packs is not expected to rise significantly over ambient when vehicles are stationary and not charging. The temperature variations during charging and driving will depend on the design of the pack and the type of cooling system and will not be considered in the model (see Section 2.4.1 of this report).